Probabilistic TSUnami Hazard MAPS
for the NEAM Region (TSUMAPS-NEAM)
ECHO/SUB/2015/718568/PREV26

PHASE I – STAGE 4: Preliminary Implementation Plan (Workflow)

Author: **TSUMAPS-NEAM Technical Integrator (TI) team**

Date: **19 June 2017**

Version: **1.0**

Table of Contents

Executive Summary

This document describes the details of the planned implementation at all STEPS.

This is the final result of the pre-assessment PHASE in which a larger number of alternatives have been 'trimmed' as a result of the first elicitation STAGE.

The Levels within each of the four STEPS which compose the SPTHA have already been introduced in Section 2.5 of DOC_P1_S1.

This document is organized into two parts.

The first part reports a more detailed explanation of the Levels, specifically defining the assessment to be performed at each of the Levels. That is, in this part we specify what we want to do.

The second part presents the alternatives selected for implementation at each Level, with some technical detail. That is, in this part we specify how we want to do it.

Altogether, the two parts of this document constitute the Preliminary Implementation Plan of TSUMAPS-NEAM SPTHA.

This page is intentionally left blank.

1. Detailed explanation of the Levels for STEPs

From document *Doc_P1_S1_ProjectSummary*, we recall that the four STEPs of the assessment in TSUMAPS-NEAM are:

- STEP 1: PROBABILISTIC EARTHQUAKE MODEL
- STEP 2: TSUNAMI GENERATION & MODELING IN DEEP WATER
- STEP 3: SHOALING AND INUNDATION
- STEP 4: HAZARD AGGREGATION & UNCERTAINTY QUANTIFICATION

In this section, we describe in more details with respect to the *Doc_P1_S1_ProjectSummary* the different Levels composing these four STEPs. At each Level, we specifically define what needs to be quantified. The methods with alternatives used for these quantifications will be described in *Section 2*.

At each STEP, Level 0 defines data and definitions required for the assessment. Levels starting from 1 define actual actions undertaken within the assessment.

1.1 STEP 1 - PROBABILISTIC EARTHQUAKE MODEL

At STEP 1 we have defined three Levels (0-2). A branching exists for Level 2 that is split into Level 2a and 2b.

The general aim of STEP 1 is definition of a list of scenarios $\{\sigma_k\}$ for all potential earthquakes in all source regions and quantification of their mean annual rates $\lambda(\sigma_k)$.

From document *Doc_P1_S1_ProjectSummary*, we recall that the Levels for STEP 1 are:

- Level 0: Regionalization, Definition of the Predominant Seismicity (PS) sources, Seismic datasets.
- Level 1: Magnitude-frequency distribution for each region including splitting of seismic activity into Predominant Seismicity (PS) and Background Seismicity (BS).
- Level 2a: Variability of PS earthquakes of given magnitude including: position along the hosting 3D-curved fault and finite fault dimensions, average slip, and slip distribution.
- Level 2b: Variability of BS earthquakes of given magnitude including: location, depth, faulting mechanism, finite fault dimensions, average slip. BS sources are assumed to be planar.

Level 0, as for the next STEPs, is used for treating the databases (including possible alternatives) which are relevant for the STEP.

Next Levels at STEP 1 coincide with the Levels of an Event Tree (ET). Hence, Levels 1-2 with their branches decompose the problem into a chain of discrete conditional probabilities for aleatory variables describing the earthquakes. Each path (or branch) through the ET represents one specific combination of all the parameters and, thus, completely defines a particular scenario to be modelled in STEPs 2 and 3. The corresponding mean annual rate of this scenario can be obtained by multiplying the mean annual rate evaluated at Level 1 with conditional probabilities along the path.

The quantifications required at these Levels are described in details below.

1.1.1 Level 0 - Regionalization & Seismic Datasets

At this Level, we discuss the regionalization, the employed/available seismicity and fault datasets, and their basic processing techniques (e.g., de-clustering, determination of completeness).

The regionalization is a subdivision of the entire NEAM seismic source area into discrete regions that are as homogeneous as possible from the standpoint of dominant tectonics. Quantification of each of the STEP 1 Levels will be performed separately for each of the regions defined by the regionalization.

Rationale for splitting seismicity into PS (Predominant Seismicity) and BS (Background Seismicity) has been presented in Section 2.2 of *Doc_P1_S1_ProjectSummary.*

Seismic datasets include:

- earthquake catalogues and their seismicity attributes (including completeness levels);
- focal mechanism catalogues;
- crustal fault catalogues for BS, including geometry, mechanism, and slip rate;
- detailed fault description for PS only, including 3D geometry, mechanism, slip rate or convergence rate, seismogenic depth and seismic efficiency (coupling, defined as a mean value over the fault surface).

Earthquake catalogues are accompanied by completeness analyses compatible with the regionalization, and both complete and de-clustered versions of these catalogues are made available.

1.1.2 Level 1 - Magnitude-frequency distribution for each region

At this Level, the frequency of the different magnitudes in each region is quantified as the sum of the contribution of Predominant Seismicity (PS) and Background Seismicity (BS). *An* earthquake belongs to a region if the geometrical centre of its fault lies within this region.

The assessment consists of quantifying mean annual rates for a set of discrete magnitude intervals M_j, with reference to the defined exposure time window (50 yr), for both Predominant and Background Seismicity in region R_i, that is $\lambda_i^{(PS)}(M_j)$ and $\lambda_i^{(BS)}(M_j)$, respectively. These two quantifications correspond to the first Level of the ET (PS-1 and BS-1, respectively) as described in Section 2.5 of document *Doc_P1_S1_Project_Summary*.

1.1.3 Level 2a - Variability of PS earthquakes of given magnitude within given region

This Level is the Predominant Seismicity (PS) branch; we here consider only earthquakes modelled as occurring along major seismogenic interfaces, e.g., subduction zones. All the parameters identifying individual sources on the 3D PS structures geometry defined at Level 0 are analysed.

The PS analysis is subdivided into the 2 sub-Levels that stack on Level PS-1, that are:

- sub-level PS-2 – Positioning along the PS hosting structure and rupture area
- sub-level PS-3 – Slip distribution

At the sub-level PS-2, position and size of the rupture area are treated simultaneously. Earthquake positions on each PS hosting fault are discretized by defining a set of coordinates $\{x_c, y_c\}$ along the 3D fault geometry. Assessment consists of quantifying the probability $\Pr_i(x_c, y_c, A|M_j)$, that is, the joint probability of a fault centre x_c, y_c and a maximum rupture area A for an earthquake of magnitude M_j in the region R_i. We simplify this quantification by computing the A as a function of

magnitude M_j from scaling laws, so that $\Pr_i(x_c, y_c, A|M_j) = \Pr_i(x_c, y_c|M_j)$, since no aleatory uncertainty is modelled for A. Average effective slip can also be estimated from the same scaling law.

At the sub-Level PS-3, we model the aleatory variability of the heterogeneous slip distribution within the rupture area A. We quantify the joint probability of a slip vector field conditioned to the occurrence of an earthquake centred at $\{x_c, y_c\}$ and having rupture area A and magnitude M_j, that is, $\Pr_i(\vec{s}\,|x_c y_c, A, M_j)$. This joint probability distribution should take into account many different constrains, such as total slip, spatial correlation of slip, etc. To simplify this quantification, instead of discretizing the slip vector space and quantifying the joint probability distribution, at this Level, we adopt a Monte-Carlo approach. We build a sampling of slip distributions, propagating each equally-probable sample with conditional probability $\Pr_i(\vec{s}\,|x_c y_c, A, M_j) = 1/n$, where n is the sample size.

The total set of scenarios to be modelled for Predominant Seismicity, $\{\sigma_k\}^{(PS)}$, is composed by all combinations of regions R_i, magnitudes M_j, centers $\{x_c, y_c\}$ and all the sampled slip distributions $\vec{s}$. The corresponding mean annual rate is computed then as:

$$\lambda\left(\sigma_k^{(PS)}\right) = \lambda^{(PS)}(R_i, M_j, x_c, y_c, \vec{s}) = \lambda_i^{(PS)}(M_j)\ \Pr_i(x_c, y_c|M_j)\ \Pr_i(\vec{s}\,|x_c y_c, A, M_j)\ .$$

1.1.4 Level 2b - Variability of earthquakes of the Background Seismicity

This Level is the Background Seismicity (BS) branch; we here consider only the earthquakes modelled as occurring outside the Predominant Seismicity faults. For BS, the dominant faulting mechanism is, hence, not pre-determined as well as the spatial distribution of earthquakes. They both vary within the volume defined by a set of cells on a regular 3D grid (see Figure 2.2.4 in of *Doc_P1_S1_ProjectSummary*). Ruptures of the Background Seismicity are modelled as single rectangular planar faults with uniform slip distribution. We analyse all the corresponding parameters: location, depth, strike, dip, rake, and slip, identifying all individual sources. Coordinates of the fault centres are distributed along the nodes of the regular grid. Similarly to the PS case, correspondence of a BS earthquake to a particular region is controlled by the position of its geometrical centre.

The BS analysis is subdivided into the 3 sub-Levels that stack on Level BS-1, that are:

- sub-level BS-2 - spatial distribution of earthquakes
- sub-level BS-3 - depth distribution of earthquakes
- sub-level BS-4 - focal mechanisms

Note that, in order to reduce the computational effort, the aleatory variability of finite fault dimensions and slip distribution are not modelled. Instead, the average values from scaling laws are adopted

At sub-level BS-2 - spatial distribution of earthquakes - given an earthquake of a given magnitude in a given region, the geometrical centre of a fault may be at different positions. The area covered by the region is thus discretised by a regular 2D grid. The assessment consists of quantifying the conditional probability $\Pr_i(x, y)$ for each potential rupture centre $\{x, y\}$ (that are, essentially, longitude and latitude) within region R_i. Note that, differently from PS, this quantification is

assumed to be independent from the magnitude value, which is consequently omitted from the notation.

At sub-level BS-3 - depth distribution -, given an earthquake of a given magnitude in a given region at a given grid cell, the geometrical centre of a fault may be at different depth. The column of crust identified by $\{x, y\}$ is thus discretised by depth levels. The assessment consists of quantifying in each region R_i the conditional probability of these different depth levels $\Pr_i(d|M_j, x, y)$ conditioned to magnitude M_j and geographical position $\{x, y\}$.

At sub-level BS-4 - focal mechanisms -, given an earthquake of a given magnitude in a given region at a given cell and depth, various faulting mechanisms are possible. Here we analyse probabilities of different strike/dip/rake combinations for each cell. Note that these probabilities are not random but, instead, their expected PDF's are derived according to past seismicity and presence of known faults. The joint conditional probability $\Pr_i(strike, dip, rake|x, y)$ in each cell $\{x, y\}$ is quantified. Note that this quantification is assumed to be independent from magnitude and depth, which are consequently omitted from the notation.

The total set of scenarios to be modelled for Background Seismicity $\{\sigma_k\}^{(BS)}$ is composed by all combinations of regions R_i, magnitudes M_j, positions $\{x, y\}$, depths d and focal mechanisms $\{strike, dip, rake\}$. The corresponding mean annual rate is then computed as:

$$\lambda\left(\sigma_k^{(BS)}\right) = \lambda^{(BS)}\left(R_i, M_j, x, y, d, strike, dip, rake\right) = \lambda_i^{(BS)}\left(M_j\right) \Pr_i(x, y) \Pr_i(d|M_j, x, y) \Pr_i(strike, dip, rake|x, y).$$

1.2 STEP 2 - TSUNAMI GENERATION & MODELING IN DEEP WATER

At STEP 2 we have defined 4 Levels (0-3).

The general aim of STEP 2 is calculation of tsunami wave time series (mareograms) at each offshore Point of Interest (POI) corresponding to the earthquake scenarios $\{\sigma_k\}$ defined at STEP 1. The logical sequence of Levels in STEP 2 is straightforward, and there is no any branching at this step.

From document *Doc_P1_S1_ProjectSummary*, we recall that the Levels for STEP 2 are:

- Level 0: Crustal elastic model; Topo-bathymetric datasets and digital elevation models
- Level 1: Co-seismic displacement model
- Level 2: Tsunami generation model
- Level 3: Tsunami propagation (in deep water) model

Level 0 is used for treating the databases (with also possible alternatives) which are relevant for this STEP.

Levels 1-3 in STEP 2 is the sequence composing the tsunami modelling from generation to propagation in deep water, up to the offshore POIs distributed along the 50 m isobaths.

The quantifications required at these Levels are described in details below.

1.2.1 Level 0 - Crustal elastic model; Topo-bathymetric datasets and digital elevation models

At this Level, we treat the choice of the: crustal models employed for calculation of the co-seismic surface displacement; topo-bathymetric databases, and the preparation of the digital elevation model on a grid (the topo-bathymetric grid) used for subsequent tsunami numerical modelling.

1.2.2 Level 1 – Co-seismic displacement model

The seafloor displacement is here modelled for each earthquake scenario $\{\sigma_k\}$ defined by the sampling at STEP1.

1.2.3 Level 2 - Tsunami generation model

This is the step where the tsunami initial condition are derived starting from the seafloor deformation obtained at the previous Level.

1.2.4 Level 3 - Tsunami propagation (in deep water) model

Here, the tsunami simulations are performed, according to the initial condition from the previous Level. The tsunami waveforms (mareograms) at the offshore POIs (Points Of Interest) corresponding to each scenario $\{\sigma_k\}$ are computed. Principle wave parameters necessary for the application of the amplification factors method (Section 2.3 *Doc_P1_S1_ProjectSummary)* including maxima, period and polarity are also extracted and stored for subsequent usage in STEP 3.

1.3 STEP 3 - SHOALING AND INUNDATION

At STEP 3 we have defined 4 Levels (0-3).

The general aim of STEP 3 is calculation, starting from the mareograms of STEP 2, of probabilities of exceedance for different hazard thresholds, conditioned to the occurrence of the scenarios $\{\sigma_k\}$ defined at STEP 1. This includes the aleatory variability introduced by the tides and the uncertainty on the hazard metric.

From document *Doc_P1_S1_ProjectSummary*, we recall that the Levels for STEP 3 are:

- Level 0: Topo-bathymetric datasets and digital elevation models
- Level 1: Amplification and inundation model
- Level 2: Tidal stage model
- Level 3: Uncertainty modelling for tsunami hazard metrics (including uncertainties from modelling approximations at STEPS 1-3, and tides).

Level 0 is used for treating the databases which are relevant for the STEP.

Level 1 deals with the estimation of coastal and / or inland tsunami hazard intensity from offshore numerical simulations at STEP 2.

Level 2 deals with the calculation of tidal stages.

Level 3 deals with uncertainty modelling and propagation at STEPs 1-3: from source to the hazard intensity metric. It can be done through the construction of PDF's for various uncertainty sources, and combination with tides. As anticipated in *Doc_P1_S1_ProjectSummary*, this part of the analysis is still under discussion.

The quantifications required at these Levels are described in details below.

1.3.1 Level 0 - Topo-bathymetric datasets and digital elevation models

Here we treat the choice of the: digital elevation model on a grid (the topo-bathymetric grid), or along 1D profiles, used for the subsequent estimation of the coastal / inland hazard intensities.

1.3.2 Level 1 - Amplification and inundation model

At this Level accepted tsunami hazard intensity metrics are computed by extrapolation of the offshore tsunami intensities stored at the end of STEP 2 (maxima, periods, polarities) to the coast / inland.

1.3.3 Level 2 - Tidal stage model,

The tidal stage time series, and their probability distributions, are evaluated at the respective POIs.

1.3.4 Level 3 - Uncertainty modelling for tsunami hazard metrics (including stochastic modelling of unmodelled effects from STEPS 1-3, and tides)

Here we model the probability of exceedance of predefined thresholds for the accepted hazard intensity metric, for each scenario and each possible combination with tidal stages. By doing this, we also need to account for uncertainties which may arise at the previous STEPs due to different model approximations and non-modelled effects. To do this, we need to quantify and sample the distributions describing the epistemic uncertainty associated with tsunami modelling.

1.4 STEP 4 - HAZARD AGGREGATION & UNCERTAINTY QUANTIFICATION

At STEP 4 we have defined 4 Levels (0-3).

The general aim of STEP 4 is quantification of hazard curves at POIs that is the exceedance probability of a chosen hazard metric within a given time window. This is done by the aggregation of the probabilities of STEP 3 according to the mean annual rates $\lambda(\sigma_k)$ of the individual scenarios $\{\sigma_k\}$ from STEP 1, and according to the weights of the alternatives models, within an ensemble modelling treatment of uncertainties. This STEP includes also comparison with observations and disaggregation analysis.

From document *Doc_P1_S1_ProjectSummary*, we recall that the Levels for STEP 4 are:

- Level 0: Elicitation of experts, historical tsunami DB, paleo-tsunami DB
- Level 1: Combination of STEPS 1-3
- Level 2: Quantification of uncertainty
- Level 3: Comparison/test with tsunami records; disaggregation

Level 0 is generally used at all STEPS for treating the databases which are relevant for the STEP. In this specific case it deals with definition of weights for the alternative models (via expert elicitation).

Level 1 deals with hazard aggregation from the previous STEPS.

Level 2 deals with concrete uncertainty estimation.

Level 3 deals with comparison with observations and disaggregation of the results.

The quantifications required at these Levels are described in details below.

1.4.1 Level 0 - Elicitation of experts

The relative credibility of alternative implementations is quantified by means of weights. The assessment consists of the quantification of w_{mnl} where m represents a given alternative model of STEP n and Level l. These weights are subjective and will be quantified through a structured elicitation experiment by the Pool of Experts (PoE). This experiment will be performed considering all the alternatives planned at all the STEPs and Levels, keeping STEPs and Levels separated (whenever possible).

1.4.2 Level 1 - Combination of STEPS 1 to 3

The contributions of all sources to the hazard at each POI are aggregated, considering the mean annual rate of each source (STEP 1), the generation and propagation in deep water of the consequent tsunami (STEP 2) and its inundation (STEP 3). The assessment consists of quantifying the hazard curves in terms of mean annual rates of exceedance of a hazard threshold for the accepted tsunami intensity metric H $\underset{mn}{\lambda}(H \geq H_k; POI, \Delta T)$ at each POI (as defined in STEP 2) for all predefined threshold values (as defined in STEP 3).

1.4.3 Level 2 - Quantification of uncertainty

All the alternative implementations at Level 1 are used on input to the Ensemble Modelling procedure to produce, for each target point, an ensemble distribution that quantifies both aleatory and epistemic uncertainty. In particular, all the annual rates $\underset{mn}{\lambda}(H \geq H_k; POI, \Delta T)$ are first transformed into $\underset{mn}{Pr}(H \geq H_k; POI, \Delta T)$ and then they form an input to produce an ensemble distribution that quantifies simultaneously all uncertainties and represents the community distribution of the resulting hazard curves (SSHAC 1997; Bommer 2012; Marzocchi et al. 2015).

1.4.4 Level 3 - Comparison/test with tsunami records; disaggregation

The results of Level 1 are used for production of secondary results. Since TSUMAPS-NEAM Project has a regional scope, the main purpose of this Level is to test the compatibility of results with available data as well as to provide general indications to be used as input and/or comparison for future analyses.

2. Alternative modeling and critical choices

In this section, we detail the implementation plan regarding alternative modelling of all the STEPs and their Levels for epistemic uncertainty quantification in TSUMAPS-NEAM.

To trim the potentially huge number of alternatives in order to focus on the most significant uncertainty-drivers, we performed the elicitation described in document *Doc_P1_S3_Elicitation*. Here, we present our implementation plan that accounts for the requests of the Pool of Experts (PoE) emerging from the elicitation and also respects practical constrains imposed by the project.

In each STEP and each Level, we summarize the PoE suggestions, our choices in response, and an overview of the alternative models to be implemented. Further technical details will be reported in the next review round. Some details need in fact to be still addressed; and some likely minor changes may be expected to happen during actual implementation.

2.1 STEP 1 - PROBABILISTIC EARTHQUAKE MODEL

The PoE elicitation recommended to implement alternatives at STEP 1 (question Q1 in Doc_P1_S3_Elicitation).

According to the question Q2 (*Doc_P1_S3_Elicitation*), alternative models are recommended for:

- Level 0: selection of the PS interfaces to be modelled separately
- Level 1: quantification of the magnitude-frequency relation

Alternatives or sensitivity tests are also suggested for:

- Level 0: tectonic regionalization
- Level 0: seismic catalogue(s) considered
- Level 2a: models for spatial distribution on PS-interfaces
- Level 2a: models for slip distribution on PS-interfaces

Alternatives and sensitivity tests can be avoided for all Level 2b sublevels.

In the next sub-sections, we discuss the implementation plan for all STEP1 levels and sublevels.

2.1.1 Level 0 - Regionalization & Seismic DBs

The PoE elicitation recommended alternatives for the selection of the PS interfaces. Additionally, alternatives or sensitivity tests were suggested for the regionalization and seismic catalogue.

As far as the PS interfaces are concerned, we opted for a different strategy. Instead of using alternatives for the selection, we added as much as possible further well-known PS sources, compatibly with the project resources available for them (creating further meshes, calculating the displacements, performing linear combinations, etc.). That is, we increased their total number with respect to those presented to the PoE at the Kick-off meeting. Additionally, we plan sensitivity tests with respect to inclusion / exclusion of PS sources. If feasible, we will perform also sensitivity tests to the PS geometry and mechanism.

The introduction of an alternative regionalization model seems instead very difficult to be accomplished within the project resources. Most likely, the second regionalization will be left for a future update of the TSUMAPS-NEAM assessment.

Finally, we plan a total of two alternative methods to assign the observed seismicity either to PS or BS sources, for discriminating the relative proportion of seismic rates and the PDFs of the faulting mechanism in a region.

The rationale behind all these choices is explained below together with a more detailed description of the implementation.

Regionalization

TSUMAPS-NEAM will adopt the regionalization specifically realized for the project, which is presented in Figure 2.1.

A second, suitable regionalization could be instead obtained by extending the EU SHARE project (http://www.share-eu.org/) zonation to the whole TSUMAPS-NEAM source region. The SHARE regionalization was specifically designed for seismic hazard in Europe, so it does not include several offshore tectonic regions, particularly along the coasts of northern Africa and in the Black Sea (see, e.g., http://portal.share-eu.org:8080/opencms/opencms/share/model/Area-Source-Model.html).

The TSUMAPS-NEAM regionalization is a subdivision of the entire source space relevant for the NEAM region into as homogeneous as possible regions, based on the dominant tectonic process acting within them. Following basic principles of plate tectonics and building on previous experience of the SHARE project (Delavaud et al., 2012), the following eleven tectonic settings are defined:

1 Active volcanoes;
2 Back-arc and orogenic collapse;
3 Continental rift;
4 Oceanic rift;
5 Contractional wedge;
6 Accretionary wedge;
7 Conservative plate boundary;
8 Transform faults s.s.;
9 Shield;
10 Stable continental region;
11 Stable oceanic region.

Region type #1 is not considered and region type #9 is not encountered. See map on Figure 2.1 (top) for the distribution of the tectonic settings defined for the NEAM region, already presented in *Doc_P1_S1_Project_Summary*, Section 2.2.

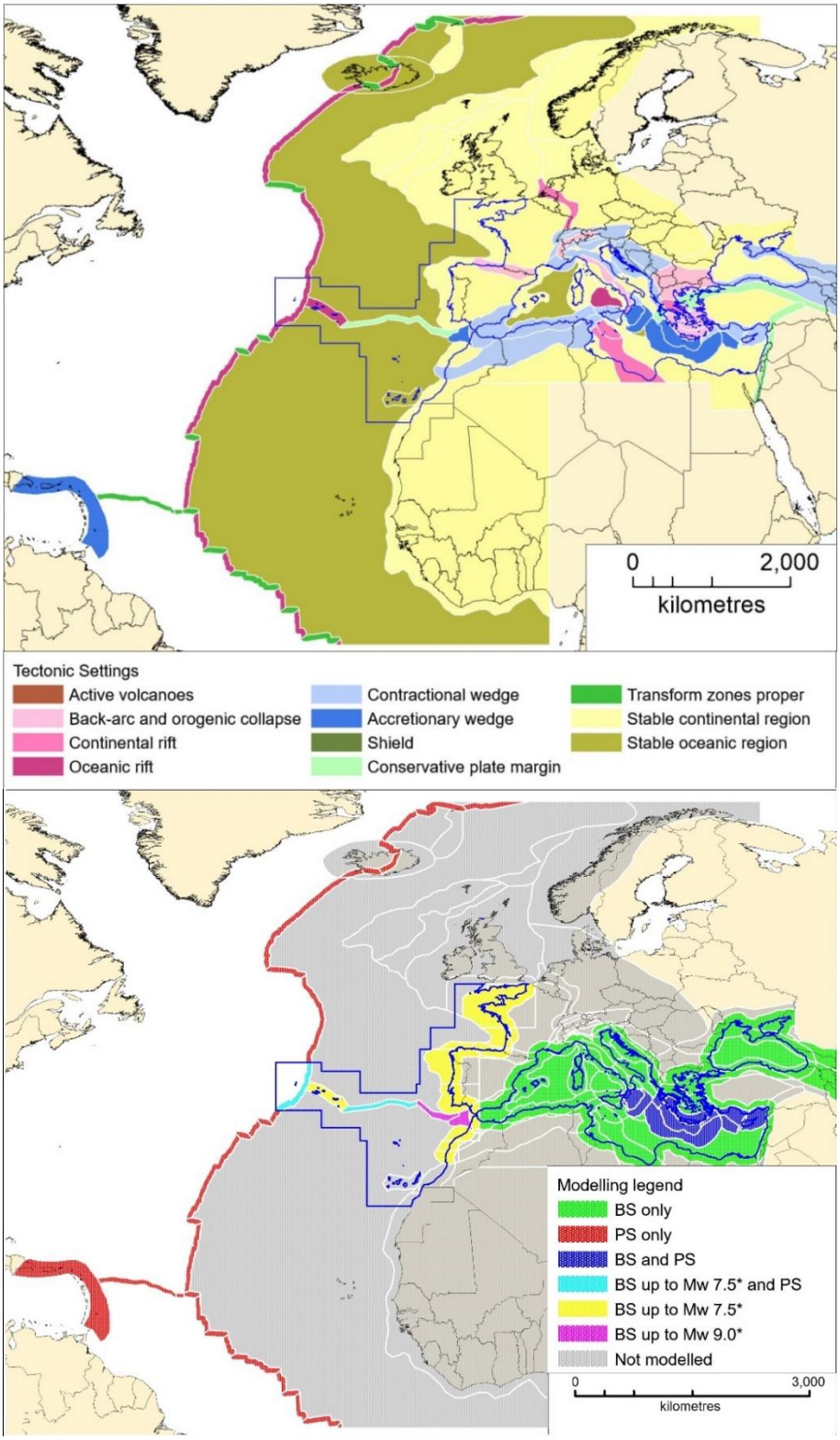

Figure 2.1 Map of the regions, colour coded depending on the tectonic setting (top) and colour coded depending on the modelling type (bottom) in the whole source area. The domain of Gaussian unit sources (blue outline) is also indicated in both maps. Asterisks '*' indicate that in some regions the computational cost of tsunami simulation imposes a hard threshold to the upper magnitude value that can be modelled, as explained in *Doc_P1_S1_Project_Summary* and later on in this document.

Seismic DBs

TSUMAPS-NEAM will adopt only one seismicity catalogue. This is obtained by merging two existing catalogues. After scrutiny of the time and geographic coverage of the largest and most authoritative catalogues available in the recent literature, we decided to adopt the ISC (ISC, 2014) catalogue for the area of the Atlantic Sea (time span 1900-2015) and the SHEEC-EMEC catalogue (Stucchi et al., 2012; Grünthal & Wahlström, 2012) for the area of the Mediterranean and connected seas (time span 1000-2006).

A statistical completeness analysis of these catalogues was performed by considering macro-regions, resulting from combinations of the individual regions in the regionalization (Figure 2.2). Other alternative seismicity catalogues will be used only for consistency checking, such as the catalogue for Mw≥7 recently compiled by NOA and the ISC-GEM historical catalogues (Storchak et al., 2013) for large magnitude earthquakes. If feasible, other sources of information will be collected.

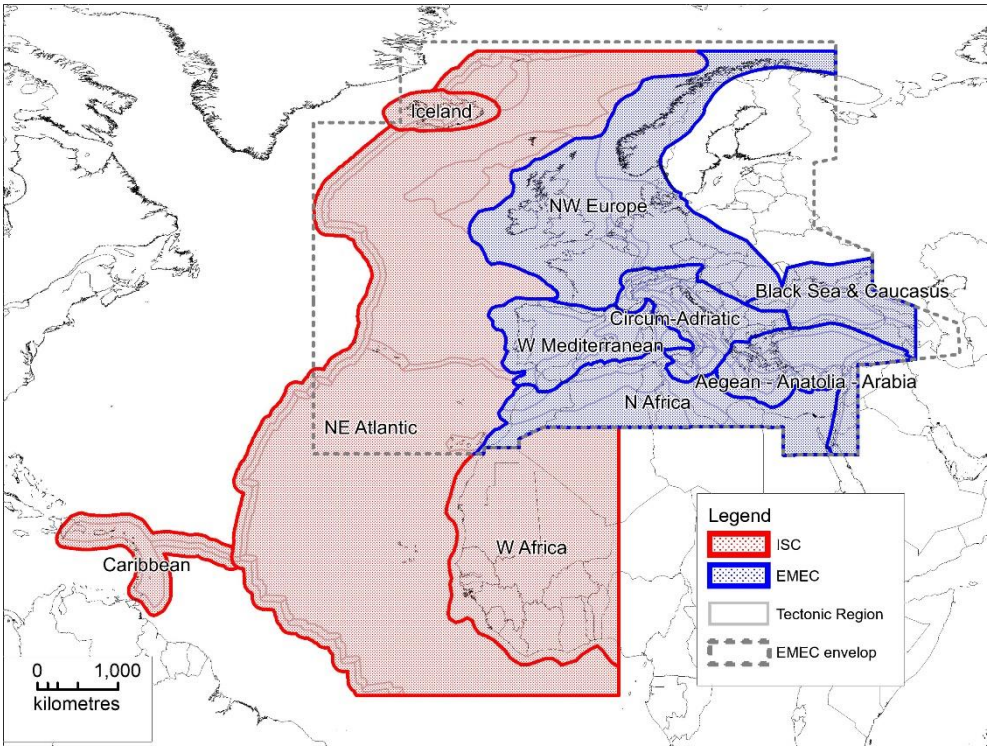

Figure 2.2. Map showing the regions used for the completeness analysis in relation with the adopted earthquake catalogues. Notice the outline of the availability of the EMEC catalogue.

TSUMAPS-NEAM will adopt only one catalogue of focal mechanisms. Considering the geographic coverage, we will adopt the global CMT catalogue (Dziewonski et al., 1981; Ekström et al., 2012) for the area of the Atlantic Sea and the RCMT catalogue (Pondrelli & Salimbeni, 2015) for the area of the Mediterranean and connected seas.

All these catalogues will be separated in two parts: PS-only and BS-only catalogues. This will be done by adopting two alternative procedures, by using two different cut-off distances of 5 and 10 km.

These two alternatives will affect all the levels of STEP 1 where data from these catalogues are used. In addition, this imposes that once a cut-off is selected at level 0, the alternatives at the following levels will be forced to be compatible (see discussion in Section 1.4, above).

We prefer to use this hard-threshold cut-off method over methods using a softer cut-off (e.g., a weighting function), for two main reasons: first, the definition of a weighting function would contain a weight-with-distance rule, which would add a further subjective choice; second, and more importantly, the Boolean separation induced by the cut-off distance allows for a smoother implementation of all models at the following levels, since it provides alternative but clearly separated catalogues of PS and BS events, instead of one single catalogue with uncertain attribution to PS/BS. The latter would have required the development of specific methods that we prefer to avoid, in order to reference (when possible) to standard and tested methodologies.

All the catalogues are also declustered adopting the Gardner and Knopoff (1974) method. The adoption of the declustered or not-declustered catalogue version will be commented in what follows at each implementation.

Fault catalogue and Predominant Seismicity (PS) selection

Fault catalogues are used as information source in combination with the CMT catalogue in two ways: for assigning the PDFs for the BS fault geometries (at sub-level BS-4 of Level BS-1, see Section 1.1.4); and for constraining the PS sources.

TSUMAPS-NEAM will adopt the European Database of Seismogenic Faults (EDSF; Basili et. al, 2013) compiled in the framework of the EU project SHARE. EDSF covers mainly the Mediterranean, the Gulf of Cadiz, and the southern part of the Black Sea. Outside these regions, i.e. most of the North Atlantic, we resorted to additional data and developed our own fault models. We used the plate boundary model by Bird (2003) as the starting reference for the Gloria fault and of the Mid Atlantic Ridge. We also used some additional information for some PS sources, such as Maesano et al. (2017) for the Calabrian Arc, and Hayes et al. (2012) for the Caribbean Arc.

According to our PS fault selection criteria (*Doc_P1_S1_Project_Summary*), we selected the following tectonic structures to be treated as PS (see also Figure 2.1):

- In the Mediterranean:
    - Calabrian Arc (subduction interface)
    - Hellenic Arc (subduction interface)
    - Cyprus Arc (subduction interface)
- In the Atlantic:
    - Gloria fault (crustal fault)
    - Mid-Atlantic Ridge (crustal faults)
    - Caribbean Subduction (subduction interface)

Project resources do not allow for considering further PS sources, such as for example the North Algerian thrust margin, neither allow for considering alternative descriptions of the selected sources. Selected PS faults are divided into the two classes (subduction interfaces / crustal faults) since the assignment of seismicity distribution between PS and BS will be treated slightly differently, as discussed later.

As said at the beginning of this Section, we prefer not to consider any alternative in the selection of PS faults. Provided that the knowledge of the modelled fault is good enough, its inclusion decreases potential significant biases in the hazard. Hence, rather than considering alternative sets of PS sources, we maximise their number.

Indeed, inclusion of one fault allows for considering much more information limiting the presence of modelled seismicity which is incompatible with the local geological and structural setting, given the sensitivity of tsunamis to the fault position, 3D fault geometry and mechanism.

Spurious sources may indeed alter the overall PSHA results (Selva et al., 2016, Selva et al., 2017). We have anyway performed some testing of the sensitivity of individual tsunami scenarios to these fault parameters (Basili et al., 2017), and to the modelling of heterogeneous slip distributions on 3D versus planar faults (Herrero et al., 2017).

Although we cannot maintain that we have a perfect knowledge of the faults that we treat as PS, adding alternative models for the fault geometry (e.g. varying the dip) would have an unaffordable computational cost for this project.

Nevertheless, we plan sensitivity tests on this issue, based on artificially reducing (or set to 0) the seismicity rate on selected PS sources. If allowed by the resources, we will also perform some further sensitivity analyses concerning how the PS geometry influences the PTHA (not only the individual tsunami scenarios). This should be anyway planned for any project update or follow up.

Convergence rate of Predominant Seismicity (PS)

In some alternative implementations described at Level 1 (next Section), to constrain the rate of activity of PS we will derive the moment rate from coupling (or seismic efficiency), rigidity (or shear modulus), fault area, and convergence rate for subduction or slip rate for other faults.

The area of each subduction zone is that of the nucleation polygon (see Sublevel PS 2). All parameters for subduction zones are derived from Davies et al. (2017) and Berryman et al. (2015). The parameters for the Gloria Fault are preliminary and those for the Mid Atlantic Ridge are yet to be defined. According to the values used for scaling laws at Levels 2a and 2b, rigidity is set to an average value of 30 GPa for subduction zones, and to 33 GPa for crustal faults (e.g. the Gloria fault) for consistency with the adopted fault scaling laws. Whether implementing depth-dependent rigidity models for subduction zones is under discussion.

2.1.2 Level 1 - Magnitude-frequency (MF) distribution

The PoE elicitation recommended alternatives for the quantification of the magnitude-frequency relation.

We describe in what follows all the implementations with their numerous alternatives occurring at Level 1.

We plan a total of 44 (8 Bayesian + 36) alternative implementations for quantifying epistemic uncertainty of MF distribution, especially on seismic rates and tails. Alternatives are planned for the shape of the distributions and their parameters, the sources of information for rates (geodetic vs seismicity), and the independence of PS and BS events.

We also plan sensitivity tests i) to check the consistency of Bayesian models with more classical MF estimation models, and ii) to quantify the probability of high magnitudes emerging from unbounded MF, for which conversely a geological limit imposed by the fault size is assumed and / or the tsunami propagation simulations would become unfeasible (modelling of a huge number of high magnitude earthquakes in the BS and their tsunamis).

Table 2.1. Tectonic data for modelling PS.

	Calabrian Arc	Hellenic Arc	Cyprus Arc	Caribbean Arc	Gloria Fault*
Nucleation area (km^2)	16008	87312	37243	TBD	17062
Convergence rate (mm/y)	1.75	10.00	6.77	11.00	4.00
b-value 1	0.70	0.70	0.70	0.70	0.70
b-value 2	0.95	0.95	0.95	0.95	0.95
b-value 3	1.20	1.20	1.20	1.20	1.20
Coupling 1	0.30	0.20	0.30	0.30	0.50
Coupling 2	0.50	0.60	0.50	0.50	0.75
Coupling 3	0.70	1.00	0.70	0.70	1.00
Mmax 1	7.60	8.00	7.70	8.00	8.30
Mmax 2	8.10	8.60	8.30	8.80	8.60
Mmax 3	9.00	9.10	9.00	9.60	8.80

* Preliminary values.

Magnitude discretization and range

As already mentioned in document *doc_P1_S1_Project_Summary*, we set M=6 as minimum tsunamigenic magnitude, meaning that in no case we model tsunamis generated by earthquakes of magnitude smaller than 6. Hence, we do not include these small magnitudes in the discretization scheme below. However, seismicity of earthquakes smaller than magnitude 6 in the catalogues contributes to the seismic rate quantification.

Magnitude discretization is performed according to Table 2.2 below. Actual intervals used for rate determination are those in the right-hand column. Tsunami modelling is performed once for each interval using the minimum value, which is the most probable (the mode) in the interval itself. In principle, if the intervals are narrow enough, these choices should not affect the results.

The sampling step gets (roughly exponentially) finer as earthquake magnitude increases; this should allow an approximately even sampling of the corresponding tsunami intensity increase, which should turn out to be approximately linear (e.g., Lorito et al., 2015).

Table 2.2. Magnitude discretization.

Nominal Magnitude	Interval represented
M_1: 6.0	[6.0000, 6.5000[
M_2: 6.5	[6.5000, 6.8012[
M_3: 6.8	[6.8012, 7.0737[
M_4: 7.1	[7.0737, 7.3203[
M_5: 7.3	[7.3203, 7.5435[
M_6: 7.5	[7.5435, 7.7453[
M_7: 7.7	[7.7453, 7.9280[
M_8: 7.9	[7.9280, 8.0933[
M_9: 8.1	[8.0933, 8.2429[
M_{10}: 8.2	[8.2429, 8.3782[
M_{11}: 8.4	[8.3782, 8.5007[
M_{12}: 8.5	[8.5007, 8.6115[
M_{13}: 8.6	[8.6115, 8.7118[
M_{14}: 8.7	[8.7118, 8.8025[
M_{15}: 8.8	[8.8025, 8.8846[
M_{16}: 8.9	[8.8846, 8.9588[
M_{17}: 8.95	[8.9588, 9.0260[
M_{18}: 9.0	[9.0260, ∞[

The maximum earthquake magnitude modelled for each BS and PS source has been chosen as follows (see also Figure 2.1).

- For all PS sources, the maximum earthquake allowed by the fault geometry and adopted scaling laws;
- for BS sources:
    - M=8.0933, corresponding to magnitude interval M_9, for the Mediterranean and connected seas;M=7.5435, corresponding to magnitude interval M_6, for all the Atlantic regions where BS has been modelled; except
    - M=9.0260, corresponding to magnitude interval M_{18}, for the Cadiz Gulf and SWIM zone.

The rationale for these limits are based on the MF global analogues proposed by Kagan et al. (2010). Most of the Mediterranean and Atlantic regions correspond to the “Active continent” and “Slow spreading ridges”, respectively, defined by Kagan et al. (2010). We thus adopt magnitude values beyond the corner magnitude obtained from the MF global estimates, which is where the rates of occurrence of higher magnitude decreases very rapidly. In the Cadiz Gulf and SWIM zone the maximum magnitude is higher because of the presence of several major faults not modelled as PS and because a subduction zone may also be present. As regards the Euro-Mediterranean region,

these magnitude values are also consistent with the annual rate decrease of the overall MF calculated by Woessner et al. (2015) for the PSHA of the project SHARE.

We thus assume that the annual rates of the higher magnitudes not modelled for tsunami propagation is negligible.

To test this, we will quantify the annual rate of all these magnitudes, as emerging from all the quantification models described below, in order to check that these values are actually negligible in terms of their influence on hazard.

Quantification of $\boldsymbol{\lambda_i^{(PS)}(M_j)}$ and $\boldsymbol{\lambda_i^{(BS)}(M_j)}$:

Two main alternatives are considered in quantifying the MF distributions for PS and BS in each region: either PS/BS distributions are quantified jointly, or independently.

For the joint PS/BS quantification, the MF distribution is quantified in two stages: in stage 1, a common MF for the region is quantified; in stage 2, the MF is split into PS and BS seismicity as a function of the magnitude (Selva et al. 2016), that is:

$$\begin{cases} \boldsymbol{\lambda_i^{(PS)}}(M_j) = \lambda_i(M_j)\,\Pr(PS|M_j, R_i) \\ \boldsymbol{\lambda_i^{(BS)}}(M_j) = \lambda_i(M_j)\,\Pr(BS|M_j, R_i), = \ \lambda_i(M_j)\left[1 - \Pr(PS|M_j R_i)\right] \end{cases}$$

where $\lambda_i(M_j)$ is the total mean annual rate of earthquakes within the region R_i having a magnitude within the interval range M_j, and $\Pr(PS|M_{j,Ri})$ represents the probability that a randomly selected event within region R_i and interval M_j belongs to the PS. Both these quantifications are based on a Bayesian formulation, with data coming from the non-declustered seismic catalogue.

For the quantification of $\lambda_i(M_j)$, we select the procedure based on the Bayesian formulation by Campbell (1982). This procedure was first suggested for the unbounded Gutenberg-Richter (GR) distribution and later refined by Keller et al. (2014) for the truncated GR distribution. The novelty of our work consists a) in extending the methodology of Keller et al. (2014) to any magnitude distribution and b) in the simultaneous estimation of all parameters. Following Keller et al. (2014), we include the temporal variability of the completeness period with magnitude, as proposed by Weichert (1980).

Both Truncated and Tapered Pareto functional forms will be considered as two alternatives. The prior distributions will be set as non-informative or slightly informative for λ_0 and Mmax/Mc (the upper limit for magnitude in the truncated Pareto and the corner magnitude of the tapered Pareto, respectively), considering all the known constraints (for example, maximum magnitude observed in the region).

Two further alternatives are planned for the parameter β (2/3 of the b-value), considering two informative priors based either on worldwide tectonic analogue estimations of Kagan et al. (2010) and a subjective "applicability index" of the worldwide analogue and the specific region, or forcing the b-value to 1. Sanity checks against more classical methods and independent databases are planned.

$\Pr(PS|M_j, R_i)$ is set as a function of magnitude, assuming that all high magnitude events must occur on PS, while events are randomly dispersed between PS and BS for low magnitudes (Selva et al. 2016). In particular, we set:

$$\Pr(PS|M_j, R_i) = \begin{cases} a(M_f) & \text{for } M \le M_f \\ a(M_f) + \left(1 - a(M_f)\right) f(M_j; M_f, M_u) & \text{for } M_f < M < M_u \\ 1 & \text{for } M \ge M_u \end{cases}$$

where M_u and M_f are the lower and upper magnitude limits for this transition, $a(M_f)$ represents the fraction of the total number of events being PS for magnitudes $M \le M_f$, and $f(M_j; M_f, M_u)$ represents a transition function. Here, we select a sigmoidal polynomial function $\mathrm{f}(M; M_f, M_u) = 3x^2 - 2x^3$ with $x = [M - M_f]/[M_u - M_f]$. Following this formulation, $\Pr(PS|M_j)$ depends on 3 parameters: M_u, M_f and a, that will be quantified as it follows separately in each region R_i.

For coherence with the MF model above, a Bayesian procedure is planned also for quantifying $\Pr(PS|M_j, R_i)$.

- For M_f, we plan to use a uniform distribution between magnitude 5 and 6.
- For M_u,, we plan to use a uniform distribution between 6 and 7 for PS relative to crustal faults, and between 7 and 8 for PS relative to subduction interfaces.
- For the parameter $a(M_f)$, we plan to set a non-informative prior (uniform between 0 and 1) updated by the measured fraction of PS events in the region in the seismicity catalogue. Given that at Level 0 we defined two alternative PS-only seismicity catalogues (different cut-off distances), two alternative implementations emerge for the fraction of PS events below magnitude M_f.

These choices produce a total of 2x4 = 8 Bayesian alternative implementations for the joint PS-BS quantification of the FM distribution, with 2 alternative shapes (tapered vs truncated Pareto), 2 b-values (from data or set to 1), and 2 PS fractions (from the different cut-off distances of Level 0). All of them are Bayesian, so that they automatically include the epistemic uncertainty emerging from parameter estimations.

For the separate PS-BS quantification, the FM distribution for PS is set as in Davies et al. (2016). This means that for constraining the rate of activity of PS we will use the classical formulation for seismic moment rate $\dot{m}_s$ as given by

$$\dot{m}_s = \chi \dot{m}_g = \chi \mu A \dot{D}$$

where $\dot{m}_g$ is the geologic moment rate, χ is a coefficient that determines how much of the geologic rate is converted into the seismic rate (so called coupling or seismic efficiency), μ is the rigidity or shear modulus, A is the fault area, and $\dot{D}$ is either convergence rate for subduction or slip rate for other faults. The area of each subduction zone is that of the nucleation polygon (see Sublevel PS 2).

Following Davies et al. (2016), and using the data reported in Table 2.1 at Level 0, we define several alternative implementations. They are: the average geodetic rate (from Berryman et al., 2015), 3 alternatives for maximum magnitudes, 3 alternative estimations for the b-value (0.7, 0.95 and 1.2) on all source zones, and 3 alternative estimations for the seismic coupling (from Berryman et al.,

2015 + coupling 0), resulting with a total of 3x3x4=36 alternatives. For BS, one of the models above is randomly sampled, independently from the PS model.

These models come with two main sensitivity tests, regarding the consistence with more classical methods. In addition, considering the upper limits in the magnitudes that may be simulated, the probability of non-simulated magnitudes will be quantified, reported and discussed, in the form of a sensitivity test.

2.1.3 Level 2a - Variability of earthquakes in Predominant Seismicity – PS

The PoE elicitation (document Doc_P1_S3_Elicitation) suggested alternatives or sensitivity tests for both sub-levels of this Level 2a (sublevels PS-2 and PS-3). Sublevel PS-2 deals with the spatial distribution of individual rupture scenarios along PS faults; sublevel PS-3 deals with slip distribution models.

We plan a total of 12 alternative implementations to explore the corresponding epistemic uncertainty. The alternatives arise from 6 different ways of distributing the seismicity on the PS sources, and from 2 alternative scaling laws. Sensitivity tests are planned for the definition of the stochastic slip distribution sampling size. Only one implementation is considered but with a variable number of asperities for each stochastic slip distribution (1 to 4 asperities), and a sensitivity test against uniform slip is performed.

We are presently also discussing (as already mentioned in *doc_P1_S1_Project_Summary*) how and whether implementing an alternative model with depth-dependent rigidity in subduction zones. This would perhaps mimic the possibility of enhanced slip towards the trench, as observed in some tsunami earthquakes and in some great megathrust earthquakes. Note that other peculiar types of tsunamigenic earthquakes, such as the outer-rise events, are allowed for occurring around the PS sources within the BS, even if they are not explicitly treated.

We first describe the discretization of the PS interfaces. Then we describe the planned implementations for both the *PS-2 and PS-3* sublevels of Level 2a.

Discretization of PS interfaces

PS faults are present only in a limited subset of regions, as reported in Figure 2.1. Note that PS coexists with BS in most of these regions, with the exception of the distant source regions, such as the Caribbean and most of the Mid-Atlantic Ridge.

3D triangular meshes have been built up for the subduction interfaces of the Hellenic, the Calabrian and the Cyprus arcs (Figure 2.3). The element size was set at about 16 km, resulting in meshes containing 3104, 1072 and 722 triangular elements, respectively. The models have been produced using the Cubit mesh generator (http://cubit.sandia.org).

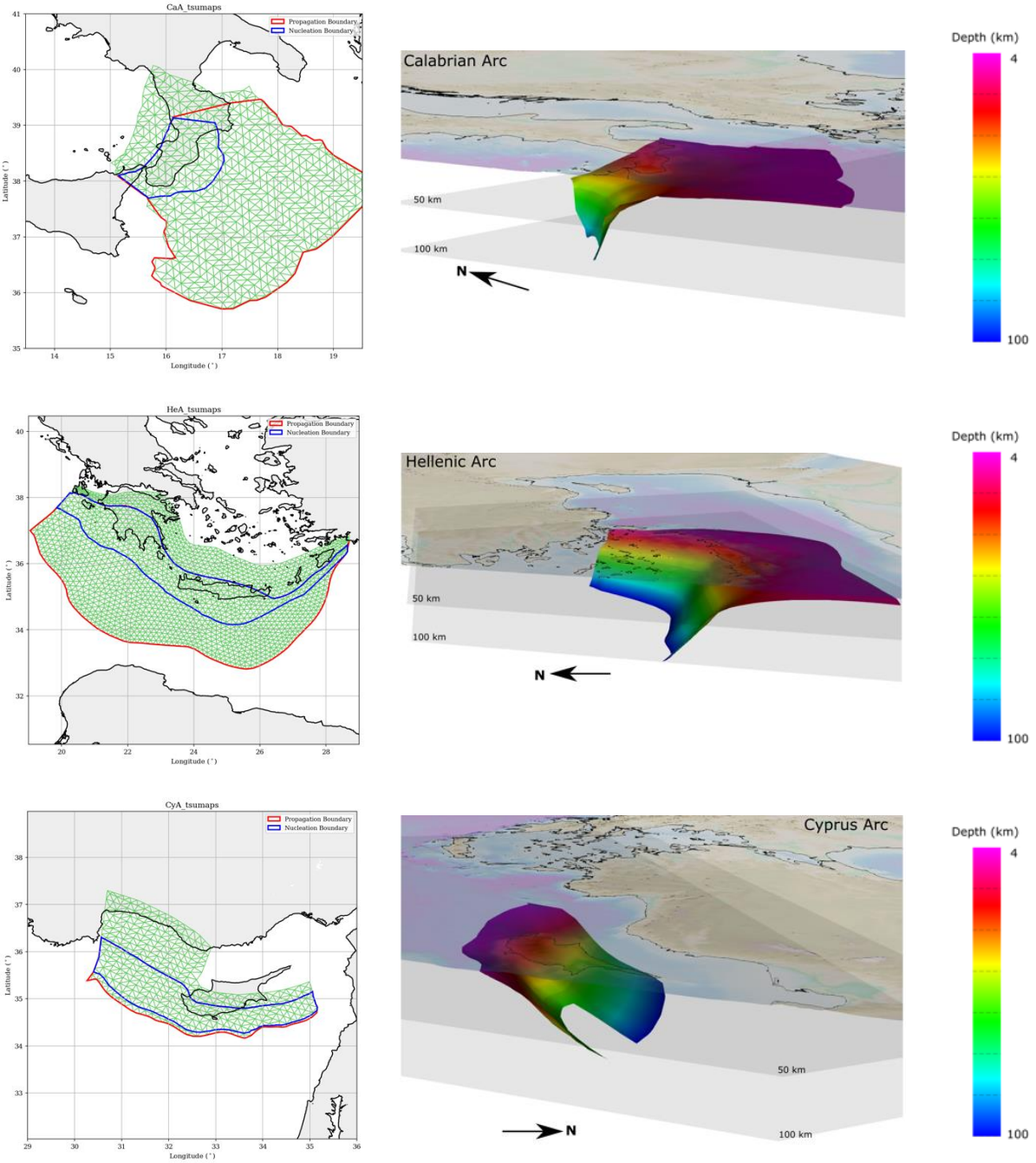

Figure 2.3 Map views of the meshes used to discretize the subduction interface in the Mediterranean region, from top to bottom (left panels) they are: Calabrian Arc, Hellenic Arc, and Cyprus Arc. The polygons which include the centres of rupture nucleation (blue) and the limits of rupture propagation (red) are also shown. 3D views of the subduction interfaces displayed with color-coded depths (right panels).

Following Selva et al. (2016) we use two alternatives for the seismogenic depth interval in the subduction zones treated as PS sources. The first alternative forces the whole earthquake slip to occur within the classic seismogenic depth interval, which we here name “nucleation zone” of each PS hosting fault. This is the zone likely dominated by unstable frictional sliding areas, mixed with relatively smaller areas of conditional stability (similar to the Domain B and C in Lay et al., 2012). The

second alternative allows for slip occurring into the “propagation zone”, the shallowest part of the PS hosting faults, where ruptures propagating updip from the nucleation zone can enter the otherwise aseismic zone due to dynamic frictional conditions controlled by sediments and fluids. The nucleation and propagation zones are those shown in Figure 2.3, enclosed by blue and red polylines, respectively.

Centres of potential earthquakes are defined inside the nucleation zone only, with the aim of uniformly covering the whole area (see Figure 2.3). Average distance between centres roughly corresponds to the size of the smallest considered earthquake with magnitude M=6.

The Mid Atlantic Ridge (Figure 2.4) was discretized into 270 rectangular subfaults; 214 of them with normal faulting mechanism, constant dip angle=45° and size 40x45 km; 56 with pure strike slip mechanism, constant dip angle=90° and size 55x20 km. The earthquake magnitude sampling can be honoured by combining a different number of subfaults (Table 2.3), since the subfault sizes are determined to make this possible according to the Leonard (2014) scaling laws.

The size of the subfaults is chosen in order to use one or more subfaults for spanning over the magnitude values of Table 2.1, starting from the minimum tsunamigenic magnitude defined for each PS zone.

For the Mid-Atlantic Ridge, earthquakes smaller than 7.3 have been tested to create negligible tsunamis along the POIs defined by TSUMAPS-NEAM along the NEAM coastlines. The only exception is where the Ridge is close enough to the POIs, such as the zone around the Azores Islands shown in close-up view in Figure 2.4, which also roughly corresponds to the cyan segment of the Mid-Atlantic Ridge in Figure 2.1. In these zone, the small PS zone earthquakes are modelled by combination of the Gaussian sources instead of using subfaults. The segment crossing Iceland will be treated in the same way.

The Gloria fault (Figure 2.5) is discretized in the same way as the Mid-Atlantic transform faults.

The discretization for the Caribbean subduction (Figure 2.6) uses the same principles, i.e. it is discretised with subfaults, but with the subfault size determined according the scaling laws for the subduction interface (Table 2.4). The magnitude range to be used for the Caribbean subduction is yet to be decided and will determine the actual discretization to be achieved that depends also on the minimum magnitude to be simulated.

Two alternative scaling laws will be adopted for the subduction interfaces treated as PS, that is those in Strasser et al. (2010) and in Murotani et al. (2013). Table 2.4 lists discretization of the relevant parameters for modelling the individual ruptures on subduction interfaces adopting the fault scaling law by Strasser et al. (2010). Figure 2.7 shows a comparison of the values listed in Table 2.4 with the values that would results by adopting other scaling laws.

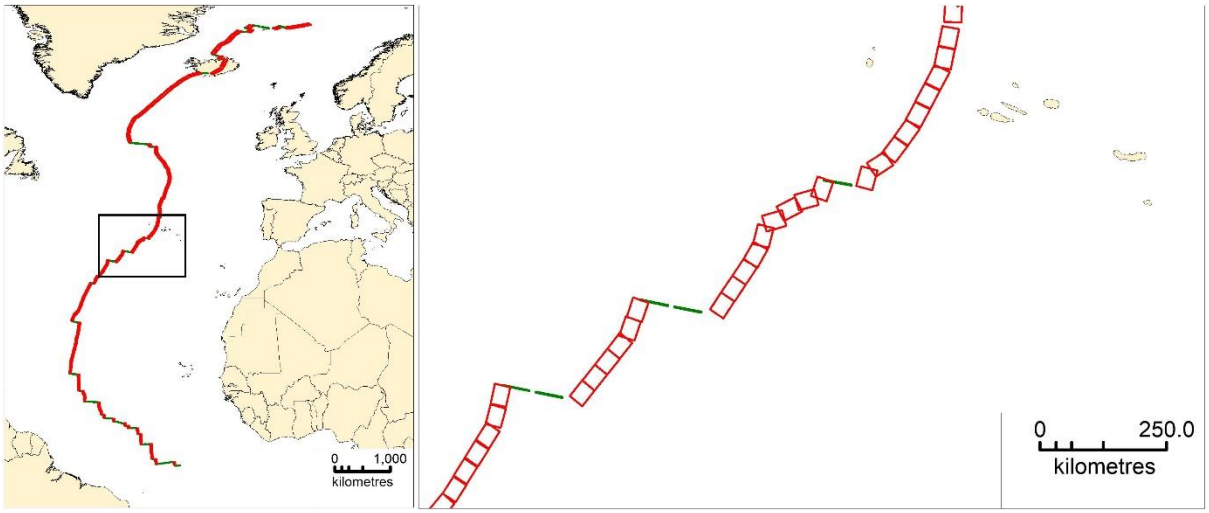

Figure 2.4 PS discretization of the Mid Atlantic Ridge (red = normal; green = transform). Right panel: distribution of all subfaults in the NEA; left panel: close-up view in the Azores (see right panel for location).

Table 2.3. Parameters of subfaults in the Mid-Atlantic Ridge zone.

A) Normal faults (spreading ridges): fixed patch size: L = 40, W = 45; total number of patches = 214

M_w	M_0 (Nm)	L (km)	W (km)	A (km^2)	D (m)	N. subfaults	L* (km)	A* (km)	ΔA (km^2)	D* (m)	ΔD (m)
7.3203	1.22E+20	70	30	2091	1.94	1	40	1800	-291	2.25	0.31
7.5435	2.63E+20	96	37	3495	2.51	2	80	3600	105	2.44	-0.07
7.7453	5.28E+20	127	44	5563	3.17	3	120	5400	-163	3.26	0.10
7.9280	9.93E+20	163	52	8472	3.91	5	200	9000	528	3.68	-0.23

B) Strike-slip faults (transforms): fixed patch size: L = 55, W = 20; total number of patches = 56

M_w	M_0 (Nm)	L (km)	W (km)	A (km^2)	D (m)	N. subfaults	L* (km)	A* (km)	ΔA (km^2)	D* (m)	ΔD (m)
7.3203	1.22E+20	112	19	2139	1.90	2	110	2200	61	1.84	-0.05
7.5435	2.63E+20	188	19	3577	2.45	3	165	3300	-277	2.66	0.21
7.7453	5.28E+20	299	19	5692	3.09	5	275	5500	-192	3.20	0.11
7.9280	9.93E+20	455	19	8670	3.82	8	440	8800	130	3.76	-0.06

* recalculated parameter after combining subfaults

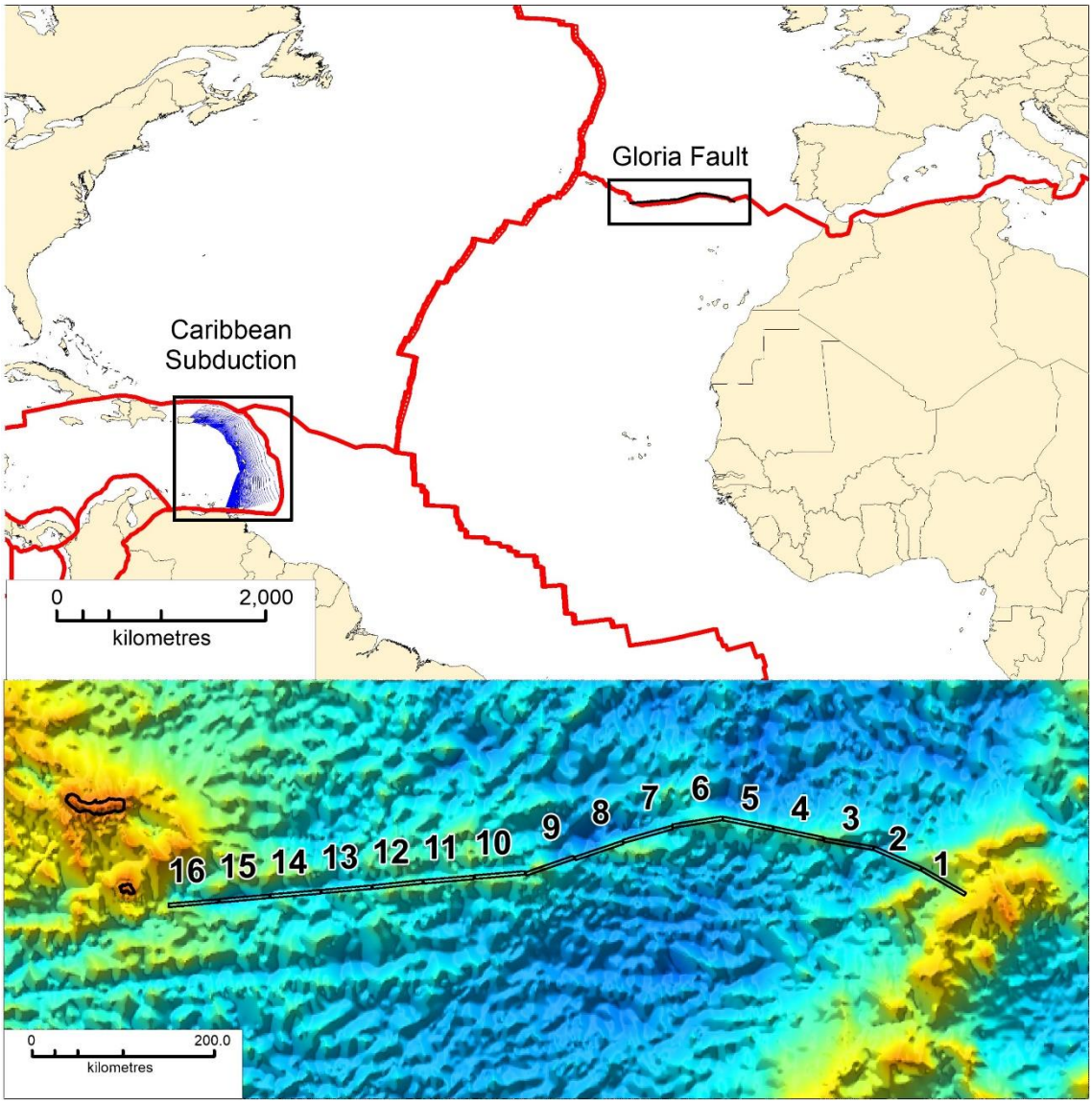

Figure 2.5 Discretization of the Gloria Fault in 16 subfaults (lower panel) whose parameters are shown in Table 2.3B. Location of the Gloria Fault (upper panel) in the Atlantic Sea context and the plate boundaries after Bird (2003).

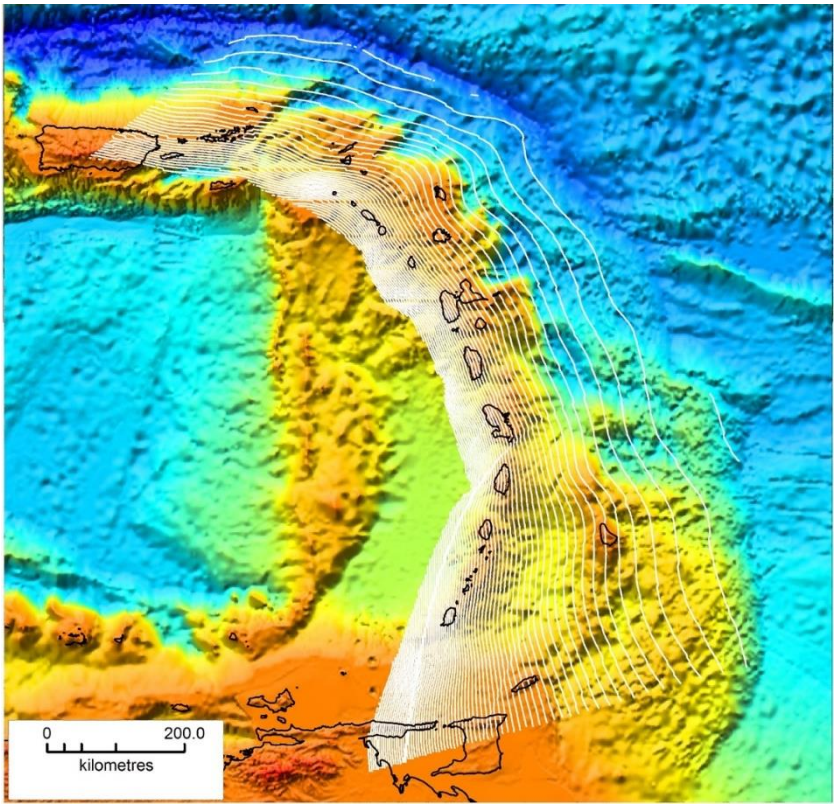

Figure 2.6 Map showing the subduction interface (white lines are contours starting at 5 km depth at the trench, with 5 km interval) from the Slab 1.0 model by Hayes et al (2012). Location shown in Figure 2.5.

Table 2.4. Slab Interface: predictions of L, W, and A by Strasser et al. (2010), as well as D derived from seismic moment and A adopting a rigidity of 33 GPa.

Mw	M_0 (Nm)	L (km)	W (km)	A (km^2)	D (m)
6.0000	1.27E+18	11	17	172	0.22
6.5000	7.16E+18	21	25	515	0.42
6.8012	2.03E+19	32	32	997	0.62
7.0737	5.19E+19	46	40	1812	0.87
7.3203	1.22E+20	64	49	3111	1.19
7.5435	2.63E+20	86	58	5075	1.57
7.7453	5.28E+20	113	69	7898	2.03
7.9280	9.93E+20	145	80	11788	2.55
8.0933	1.76E+21	181	91	16936	3.14
8.2429	2.95E+21	221	103	23509	3.80
8.3782	4.70E+21	266	114	31626	4.51
8.5007	7.18E+21	313	126	41368	5.26
8.6115	1.05E+22	364	138	52741	6.05
8.7118	1.49E+22	416	150	65710	6.86
8.8025	2.04E+22	470	161	80164	7.70
8.8846	2.70E+22	525	172	95971	8.54
8.9588	3.49E+22	581	183	112922	9.37
9.0260	4.41E+22	636	193	130843	10.20

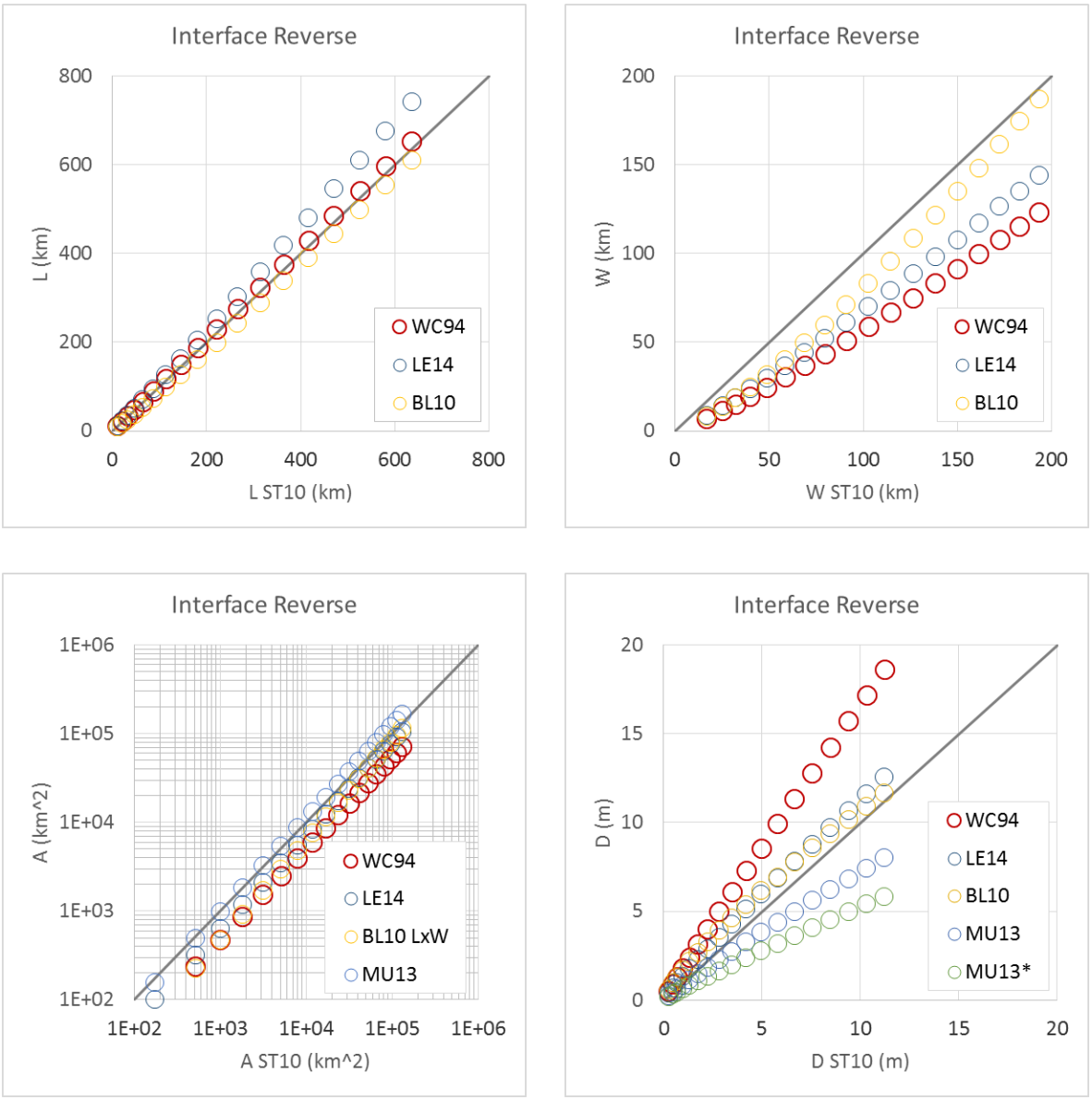

Figure 2.7. Comparison of relations by Strasser et al. (2010) (ST10) with relations by Wells and Coppersmith (1994) (WC94), Leonard (2014) (LE14), Blaser et al. (2010) (BL10), and Murotani et al. (2013) (MU13) in predicting fault length (L), width (W), area (A), and average displacement (D) in the case of dip-slip earthquakes on subduction interfaces for all Mw samples in Table 2.4. Displacement in MU13* is directly derived from the relationship, in all other cases it is derived from seismic moment, using an average shear modulus of 30 GPa and the area predicted by the relationship.

Sublevel PS-2

Quantification of: $\mathbf{Pr}_{\mathbf{i}}(x_c, y_c, A|M_j)$

The assessment consists of quantifying simultaneously position and size of the rupture area for each $\{x_c, y_c\}$ indicating the rupture centres.

For sublevel PS-2, the spatial distribution of events along the PS faults is modelled either uniformly, or it can vary along the strike proportional to the observed seismic rate. For the latter option, we will use an *ad hoc* procedure similar to the smoothed seismicity (for coherence with Level 2b – sublevel BS-2, described below). The declustered catalogue will be used, considering PS-only catalogue, as emerging from the 2 alternative cut-off distances considered at Level 0. This leads to 3 alternatives (uniform + 2 PS-only catalogues).

In all the cases, centres of ruptures are allowed only if the corresponding fault area A can be embedded into the boundaries of the PS hosting structure, that is, the distance from the edges should be larger or equal to $L/2$ laterally, and W/2 along dip, with L and W being the length and width provided by the scaling laws. From these latter relationships and for each magnitude bin the size of the mesh area actually involved in the rupture is also computed.

Two alternatives are considered in defining such boundaries, that is the "nucleation" and "propagation" zones defined above (in "***Discretization of PS interfaces***") for all PS sources. In both of the cases the centres however fall only inside the nucleation zone. However, when the model using both the nucleation and the propagation zones is used, the centres are allowed to lie closer to the shallow nucleation zone boundary, since more space is allowed updip for the rupture area. Rupture in the propagation zone is not assumed to contribute to the seismic moment balance, which is in both cases evaluated by considering only the nucleation zone area.

Since the two alternative scaling laws of Strasser et al. (2010) and Murotani et al. (2013) are used, the above procedure is repeated twice.

All these choices lead to 12 alternative implementations for computing $\Pr_{\mathrm{i}}(x_c, y_c | M_j)$.

Sublevel PS-3

Quantification of: $\boldsymbol{\Pr_i(\vec{s}\,|x_c y_c, A, M_j)}$

To build the heterogeneous slip on non-planar faults using the above-mentioned triangular mesh, the following scheme is implemented.

For each event defined by $\{x_c y_c, A\}$, the area A is iteratively covered extracting nearby cells starting from the geometric center and over this area a Probability Density Function (PDF) for the slip distribution is defined as the sum of a random number N of Gaussian functions, with $1 \leq N \leq 4$, such that the slip can represent either single or multiple asperities distributions.

Each Gaussian is defined by randomly extracting the position of the maximum from a uniform distribution and setting the standard deviation as one fifth of the square root of the rupture area, so that, when the centre is quite far from the edges the probability goes to zero well-within the rupture zone. When the centre of the Gaussian is closer to the edge, the slip has to be *a-posteriori* re-distributed accordingly with the imposed seismic moment.

Within the fault area, the slip value is assigned to each triangle using a hierarchical set of overlapping circular sub-events on the fault surface; the number of sub-events is a decreasing power-law of their radii as in the following law:

$$n(R) = pR^{-D-1}$$

R is defined in the interval $[R_{min}\ R_{max}]$ where R_{min} is fixed such that the circle covers at least five elements to ensure that the slip is everywhere well resolved by the mesh; R_{max} is fixed at 35% of the rupture width derived from the pre-computed magnitude and length. Only one asperity of maximum radius is placed, whereas the total number of cracks is fixed at 1000. D, the fractal dimension and it is set to 2 to ensure the self-similarity of the slip distributions (Herrero & Bernard, 1994), whereas the constant p is set accordingly to the moment, equal to the fractal dimension of the expected stress drop (Zheng *et al.*, 1994, Murphy *et al.*, 2016).

The precision of the circular asperities on the non-planar mesh is ensured by a double-lateration algorithm (Herrero & Murphy, SSA meeting, 2017; Herrero *et al.*, EGU meeting, 2017) derived from a multi-lateration scheme proposed by Novotni & Klein (2002). Finally, the slip distribution across the single sub-events is assigned by an Eshelby function (Eshelby, 1957; Ruiz *et al.* 2011), based on the above-described probability density function.

To mimic the smooth end of the seismogenic fault zone the centre of each single sub-event must lie at least at a distance from the edge larger than their radius. This constraint is released close to the shallower boundary: this may allow to model the shallow slip amplification due to the free surface effect. The algorithm is efficiently implemented in a Fortran code and produce a slip distribution approximately every ten seconds.

As discussed in Section 1 and in the document *doc_P1_S1_Project_Summary*, at this level we adopt a Monte-Carlo sampling procedure. The size of the sample will be defined at later stages, based on temporal feasibility and sensitivity tests. Additionally, this sampling will be limited to large magnitudes ($M > 7.5$ or $M > 8.0$, depending on the region) and to a subset of PS faults. Specific sensitivity tests will be implemented to support decisions.

As said, we are also considering the feasibility of another approach based on depth-dependent rigidity, and as a consequence a depth-dependence of slip. Heterogeneous stochastic slip on curved interfaces will be superimposed according to the average slip value.

As said at the beginning of this Section 2.1.3, only one implementation is considered but with a variable number of asperities for each stochastic slip distribution (1 to 4 asperities), and a sensitivity test against uniform slip is performed.

2.1.4 Level 2b - Variability of earthquakes in Background Seismicity – BS

The PoE elicitation (document Doc_P1_S3_Elicitation) did not recommend nor suggest alternatives for Level 2b and its sublevels.

We plan a total of 2 alternatives (with 1 Bayesian model for strike-dip-rake), exploring the epistemic uncertainty induced by BS catalogue definitions. These alternatives cannot be trimmed since they are inherited from Level 0. We do not plan any specific sensitivity tests at this level.

Since for BS we use uniform slip and the best guess for spatial dimensions from a single scaling law, we can foresee testing of this simplification in a future update of the assessment.

BS is present in most of the regions, as reported in Figure 2.1, bottom panel. The only exception is the distant source regions of the Atlantic (in red in Figure 2.1). In most of the cases, it is the only seismicity class present, and in some cases, it coexists with PS.

In the following we describe the planned implementations for both Level 2b sublevels BS-2 and BS-3.

Scaling laws for (crustal) BS sources.

As discussed in Section 1 and recalled above, fault size and average slip are set as the central value (mean) of the scaling laws and a uniform slip distribution on planar rectangular faults is assumed.

The adopted fault scaling law for the BS are those by Leonard (2014), which are based on the largest dataset of earthquake ruptures from around the world and, with respect to older scaling laws, allow for considering not only the faulting mechanism (dip slip and strike slip) but also the tectonic setting (interplate and stable continental regions). Note that these scaling laws are used also for the crustal faults treated as PS (Mid-Atlantic Ridge, Gloria fault).

Tables 2.5 and 2.6 show the earthquake magnitude sampling for crustal faults for interplate and stable continental regions (SCR), respectively. For each magnitude, the rupture area A is derived from scaling laws, and average slip <D> from the seismic moment, as $<D>=M_0/\mu A$, assuming a shear modulus μ=33 GPa.

Table 2.5. Interplate: predictions (rounded) of L, W, A, and D by Leonard (2014).

				Dip Slip				Strike Slip	
Mw	M_0 (Nm)	L (km)	W (km)	A (km^2)	D (m)	L (km)	W (km)	A (km^2)	D (m)
6.0000	1.27E+18	11	9	100	0.38	13	7	102	0.38
6.5000	7.16E+18	23	14	316	0.68	25	11	324	0.67
6.8012	2.03E+19	34	19	633	0.96	38	15	647	0.95
7.0737	5.19E+19	50	24	1185	1.31	64	19	1213	1.29
7.3203	1.22E+20	70	30	2091	1.74	112	19	2139	1.72
7.5435	2.63E+20	96	37	3495	2.25	188	19	3577	2.22
7.7453	5.28E+20	127	44	5563	2.84	299	19	5692	2.80
7.9280	9.93E+20	163	52	8472	3.50	455	19	8670	3.46

Table 2.6. SCR: predictions (rounded) of L, W, A, and D by Leonard (2014).

				Dip Slip				Strike Slip	
Mw	M_0 (Nm)	L (km)	W (km)	A (km^2)	D (m)	L (km)	W (km)	A (km^2)	D (m)
6.0000	1.27E+18	10	6	65	0.59	11	5	66	0.58
6.5000	7.16E+18	20	9	204	1.05	22	8	209	1.04
6.8012	2.03E+19	31	12	409	1.48	34	11	418	1.47
7.0737	5.19E+19	45	15	765	2.03	49	14	783	2.01
7.3203	1.22E+20	63	19	1350	2.69	76	17	1381	2.67
7.5435	2.63E+20	86	23	2257	3.48	127	20	2309	3.45
7.7453	5.28E+20	113	28	3592	4.39	202	20	3675	4.36
7.9280	9.93E+20	146	33	5470	5.42	308	20	5598	5.38

The comparison of the fault area and displacement predicted by Leonard (2014) in interplate setting and SCR setting (Figure 2.7) shows the importance of using different scaling laws in different tectonic settings. From Leonard (2014) it appears that faults in SCR are relatively smaller and have relatively higher average slip for any given earthquake magnitude.

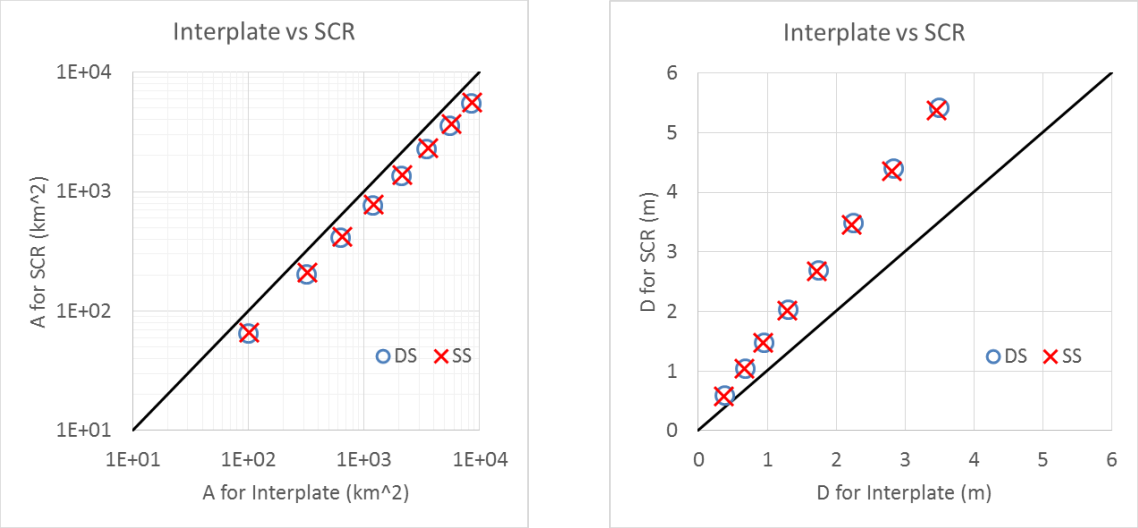

Figure 2.7. Predictions for fault area (A) and fault displacement (D) in the case of dip-slip (DS) and strike-slip (SS) earthquakes in interplate setting compared with those in stable continental region (SCR) setting using the relationship by Leonard (2014). The earthquake magnitude samples are as in Table 2.5 and Table 2.6.

Sub-level BS-2

Discretization: As shown in Section 2.2 of *Doc_P1_S1_Project_Summary*, the discretization of the spatial domain is based on a regular grid composed by non-conformal equal-area cells of 25x25 km. The centres of each grid points inside the regions in which BS is modelled represent the discretization for each region.

Quantification of $Pr_i(x, y)$:

A spatial smoothed seismicity model will be adopted, using the Nearest Neighbour (adaptive kernel) method. The declustered seismicity catalogue will be adopted, considering the BS-only catalogue, leading to the 2 alternatives arising from Level 0.

Sub-level BS-3

Discretization: The discretization of the depth domain is defined by considering different depth levels for the top of the fault. To achieve a good sampling of the volume in each cell, a different discretization of the depth is considered for each of the different magnitude levels Mj (Figure 2.8), that is:

M_1: 1.0, 3.53, 6.06, 8.59, 11.13, 13.66, 16.19, 18.72, 21.25 km
M_2: 1.0, 4.54, 8.08, 11.62, 15.15, 18.69 km
M_3: 1.0, 4.91, 8.81, 12.72, 16.63 km
M_4: 1.0, 5.44, 9.88, 14.32 km
M_5: 1.0, 6.4, 11.8 km
M_6: 1.0, 9.08 km
M_7: 1.0, 6.2 km
M_8: 1.0 km
M_9: 1.0 km

The discretization of the hypocentral depth depends on the earthquake's magnitude; we assume an average thickness of the seismogenic layer equal to 27 km.

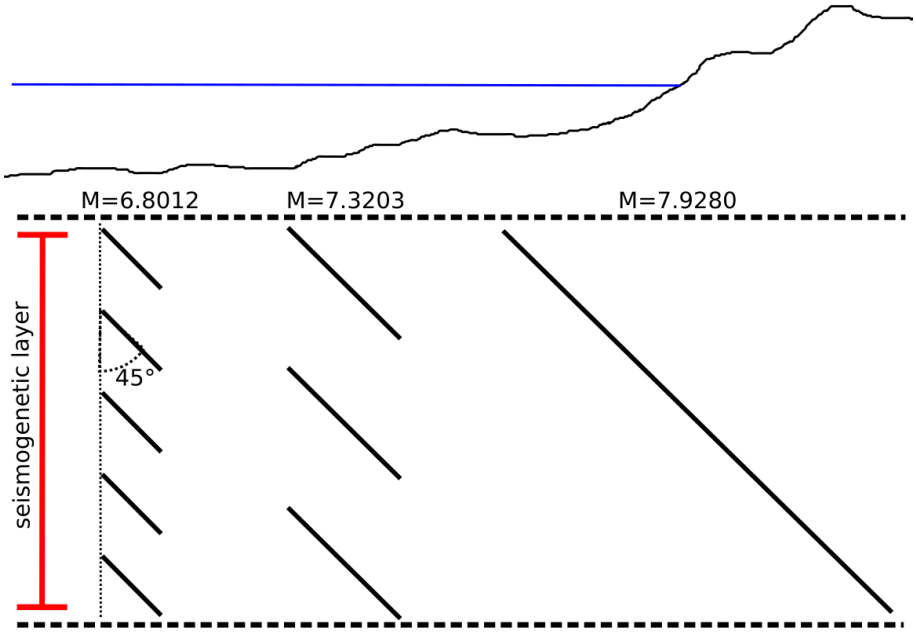

Figure 2.8 Scheme for the earthquake magnitude-dependent depth discretization for BS fault sources.

Quantification of $\boldsymbol{Pr_i(d|M_j, x, y)}$ ***:*** A uniform distribution for depths is assumed.

Sub-level BS-3

Discretization: The discretization is made separately for strike, dip and rake. To manage the toroidal properties of angles, the strike and dip transformed as it follows:

$$S = \begin{cases} strike, strike < 180 \\ strike - 180, strike > 180 \end{cases}$$
$$D = \begin{cases} dip, \ strike < 180 \\ 180 - dip, strike > 180 \end{cases}$$

With this 1-1 reversible transformation, both strike and dip range between 0 and 180, and two sub-vertical fault planes with opposite strike and dip close to 90 will have equal S and close D values. Adopting this transformation, the following discretization is adopted:

- S: 22.5, 67.5, 112.5, 157.5 (each representing intervals of 45 degrees, starting from 0 up to 180)
- D: 10, 30, 50, 70, 90, 110, 130, 150, 170 (each representing 20 degree intervals around the central values, starting from 0 up to 180).
- Rake: -90, 0, 90, 180 (each representing 90 degree intervals around the central values)

This makes a total of 4x9x4=144 combinations.

Quantification of $\underset{i}{Pr}(strike, dip, rake|x, y)$ ***:***

A Bayesian method similar to the one adopted in Selva et al. (2016) is implemented. In particular, in each region an informative prior model based on worldwide data is used that is updated with the focal mechanism catalogue available. We will consider the BS-only not declustered catalogue, and both focal planes are assumed equiprobable and included into the uncertainty quantification. The obtained regional posterior is then used as prior in each cell. If faults are present in the fault catalogue in each cell, this prior is combined to a strongly informative prior distribution based on local faults.

In all these assessments, the BS-only catalogues are considered as emerging from the 2 alternative cut-off distances considered at Level 0.

2.2 STEP2 - TSUNAMI GENERATION & MODELING IN DEEP WATER

The PoE elicitation (document Doc_P1_S3_Elicitation) did not recommend nor suggest alternatives for STEP 2 (question Q1).

Even if STEP 2 is not considered overall critical by the PoE, they pointed out that some Levels within the STEP contain some elements that are more critical than others. For example, at Level 0, the importance of the digital elevation model used for tsunami simulations has been pointed out. Similarly to other cases, repeating the tsunami simulations would be unaffordable though. Conversely, we focussed on implementing alternatives for STEPS that are considered overall more critical.

Implementation of all the levels of STEP 2 was already described in some details in document Doc_P1_S1_Project_Summary. We here add some further information on specific aspects.

Level 0 - Crustal model (elastic parameters, friction); Topo-Bathymetric datasets and digital elevation models

Crustal model: Poisson solid; elastically homogeneous crustal models.

Topo-bathymetry: SRTM30+, improved in the NE region with local data in Portugal, and in the Black Sea with SRTM15+ resampled at 30 arcsec. Both SRTM datasets are available at http://topex.ucsd.edu/WWW_html/srtm30_plus.html.

Level 1 - Coseismic displacement model

Sea-bottom co-seismic displacement associated to each scenario is computed for the BS sources and for the individual PS subfaults in the Atlantic Sea with an algorithm which solves for the static displacement due to a planar rectangular fault buried in a homogeneous Poisson's solid (Okada, 1992). A special version of this algorithm (Meade, 2007) has been used for the triangular subfaults forming the meshes for the 3D PS structures (Calabrian, Hellenic, and Cyprus Arcs).

Heterogeneous slip values are imparted to the triangles of the meshes to implement the slip distributions defined at STEP 1.

The vertical component of the displacement used as input for tsunami simulations is sampled at 30 arcsec, which is the spatial resolution of the grids used for tsunami modelling. Since Okada's analytical solution is prone to produce very long 'tails' of low-amplitude surface displacements, for practical reasons, we restrict the deformation area to vertical displacements larger than 1 cm.

Due to the extremely large number of simulated scenarios in TSUMAPS-NEAM, we do not consider any alternatives for this Level 1. Potential alternatives for this step could include, e.g., 1D layered crustal model or 3D FEM with realistic crustal structure (especially in the vicinity of the subduction zones).

Level 2 - Tsunami generation model

Since water column effectively acts as a low-pass filter when transferring sea-bottom displacements to the sea-surface, this effect also has to be modelled in order to obtain consistent initial conditions for the subsequent tsunami wave modelling.

As anticipated in *Doc_P1_S1_Project_Summary*, in order to account for the attenuation of the short wavelengths through the water column, we apply a two-dimensional filter of the form 1/cosh(kH) (Kajiura, 1963) to the static vertical seafloor deformation field calculated at Level 1. Here *k* is the wavenumber and *H* is the effective water depth taken as the average above the 4 fault corners. The filter is applied using a spatial 2D Fast Fourier Transform algorithm.

One possible alternative at this Level 2 could be a more sophisticated filtering algorithm by Nosov and Kolesov (2011) which is not restricted to the effective uniform depth but, instead, can be applied above arbitrary complex bathymetry. This algorithm, however, is much more time consuming, so we have no possibility to employ it within the limited time of the TSUMAPS-NEAM project.

Level 3 - Tsunami propagation (in deep water) model

In this Project we simulate around 50 000 000 tsunami propagation scenarios. To accomplish this task, we employ the approach of Green's functions. Two types of Green's functions are used: to model PS scenarios in the Atlantic Ocean we use the usual approach of virtual tsunamis pre-computed for a unit slip at buried elementary faults; whereas for the rest of scenarios (BS and PS) we use a new approach with Gaussian-shaped elementary sources distributed directly at the sea surface (Molinari et al., 2016). In both cases, virtual mareograms are precomputed and stored for all possible combinations of elementary sources and POIs.

We made some exceptions though, as already discussed in Section 2.2 of *Doc_P1_S1_Project_Summary*, to limit the computational cost associated with the whole project. These exceptions are based on geophysical constraints discussed at STEP 1 in this document (Section 2.1). We recall that they are: we didn't cover stable oceanic regions with Gaussians, assuming that the seismicity is low enough; for most of the Gaussians in the Atlantic, we didn't extend enough the computational domains to allow distant propagation of the magnitudes higher than 7.5, assuming that their probability is low out of the PS sources; for several PS sources, we didn't use small enough subfaults to simulate the lower magnitudes, assuming that the tsunamis associated with these

magnitudes would not significantly affect distant NEAM coastlines; for some PS sources in the Atlantic, we used subfaults instead of triangular meshes on a 3D geometry, assuming that detailed geometry of distant sources was less important; we considered everywhere M6 as the lowest tsunamigenic magnitude. As discussed at STEP 1 (Section 2.1), we plan to test the sensitivity of the hazard to some of these choices.

Final scenario mareograms are then assembled by linear combination of the virtual tsunami Green's functions using the weights calculated from the seismic source model. In the case of "slip Green's functions", these weights correspond to the scenario slip distribution, whereas in case of "Gaussian Green's functions", weights are directly computed from the initial sea surface deformation by 'filling' the initial wave profile with the Gaussians.

Pre-computed tsunami Green's functions were simulated in all cases with the Tsunami-HySEA non-linear shallow water (NLSW) GPU-optimised code (e.g., de la Asunción et al., 2013). The code has been benchmarked during several NTHMP (http://nws.weather.gov/nthmp/) benchmarking workshops. Some details of the simulation setup can be found in Molinari et al. (2016). In all cases the spatial resolution of the simulation grid is 30 arcsec; the time series are saved each 30 s. Open boundary and drying-wetting schemes at the coast are used as boundary conditions. The time-step is automatically adapted by Tsunami-HySEA to match the Courant–Friedrichs–Lewy (CFL) condition for the deepest point in the simulation grid. The duration of the simulations depends on the specific case. For the Gaussians: in the Mediterranean, 8 hours; in the Black Sea, 4 hours; in the Atlantic, 15 hours for the larger grid (SWIM source zone Gaussians, see *Doc_P1_S1_Project_Summary*), and 8 hours for the smaller grids (all the others); for individual sources simulated up to now, i.e. those on the Mid-Atlantic Ridge, 16 hours.

Scenario mareograms obtained by linear combinations exist at the POIs located offshore: at about 50 m depth. At STEP 3, offshore wave characteristics will be used for the estimation of the coastal hazard intensity metric. Our "offshore-to-onshore" transformation (see next STEP) requires an advanced set of wave parameters including wave maximum, dominant period and polarity. At the end of the present Level 2, we perform mareogram analysis to derive the necessary wave characteristics. This analysis has following steps (see also Figure 2.9):

1. find the tsunami first arrival (by variance analysis or threshold);
2. (optionally) restrict the time window to account for the 2-3 leading waves;
3. find the maximum wave amplitude and store the value (the maximum is the hazard intensity);
4. select a 2 hours' time window W centred around the maximum;
5. remove the high-frequency component of the signal by a robust LOWESS (locally weighted scatterplot smoothing; this roughly preserves the maximum);
6. find the neighbouring relative minima on the filtered waveform;
7. estimate the period of the signal from the time distance between these minima;
8. estimate the polarity of the leading wave from the trough-to-peak ratio (R), where the trough is the first relative minimum preceding in time the (positive) maximum; and the peak is the maximum itself; polarity is assumed negative if R>25%, positive otherwise.

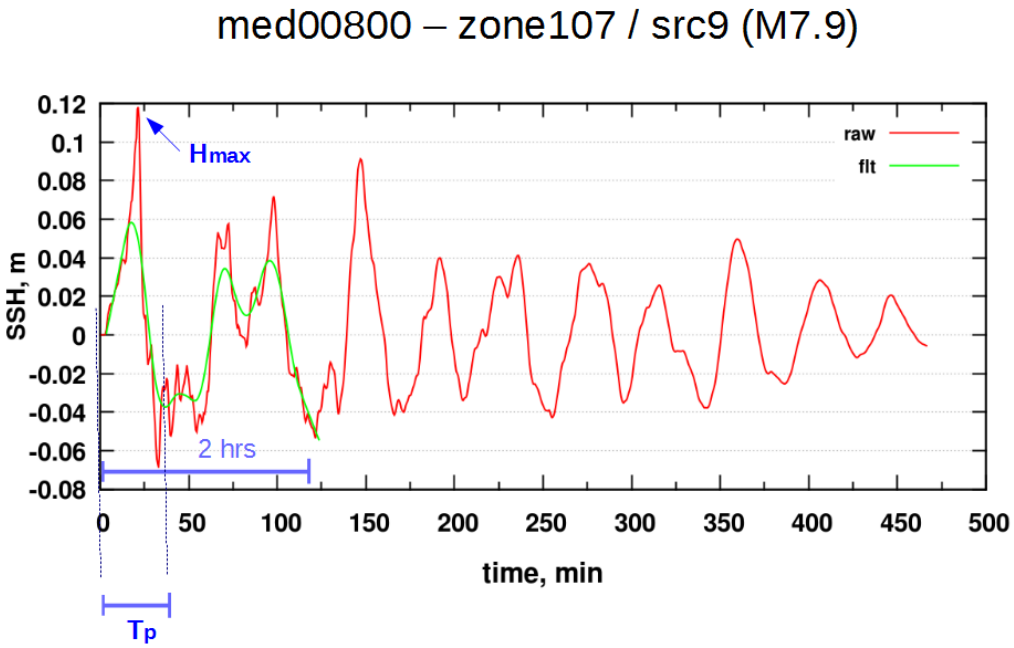

Figure 2.9 – Principles of the mareogram analysis for derivation of main wave characteristics required for the "offshore-to-onshore" transformation at STEP 3: maximum wave height, dominant wave period and polarity.

2.3 STEP 3 - SHOALING AND INUNDATION

The PoE elicitation (document Doc_P1_S3_Elicitation) recommended alternatives for STEP 3 (Question Q1).

For STEP 3 levels (question Q4), alternatives are recommended for:

- *Level 0: Topo-bathymetric datasets and digital elevation models;*
- *Level 1: Amplification and inundation model at the points of interest along the coast, and inland, corresponding to the offshore points of STEP 2;*
- *Level 3: Model the uncertainty on the tsunami metrics.*

Alternatives and sensitivity tests can instead be avoided for Level 2 (quantification of the probability for tidal stages at the points of interest).

We share the view of the PoE but unfortunately some of these alternatives are unaffordable within the project resources. We then devise a different strategy. As said in Section 2.3 of *Doc_P1_S1_Project_Summary*, along with the MIH, we will consider two alternative hazard metrics, i.e. the 'raw' offshore amplitudes at the offshore POIs, and the Green's law amplification. We will present the three types of results.

Considering that the scope of the assessment is regional, we don't need to address probabilities for local (high-resolution) inundation quantities. The above metrics are probably sufficient for regional screening of the coasts and for prioritization of local studies.

We will also estimate at this STEP the uncertainty associated with our amplification factors approach (Section 2.3 of *Doc_P1_S1_Project_Summary*).

A specific effort will be devoted to uncertainty communication to end-users.

Details of the Levels with alternatives are presented below.

Level 0: Topo-bathymetric datasets and digital elevation models

As for STEP 2, as topo-bathymetric model we use the SRTM30+ dataset improved in the NE region with local data, and in the Black Sea SRTM15+ resampled at 30 arcsec. Currently, we do not plan any alternative topo-bathymetric datasets due to the limited time and resources available to TSUMAPS-NEAM. At Level 1 of this STEP, offshore wave parameters derived at STEP 2 must be transferred into the tsunami intensity metric at the nearby coast.

As our main approach, we employ the method of local amplification factors. We then prepare here the database of coastal profiles and amplification factors as described in Section 2.3 of Doc_P1_S1_Project_Summary at all POIs, for different periods and polarities of the incident wave.

Level 1: Amplification and inundation model

The PoE elicitation (document Doc_P1_S3_Elicitation) did recommend alternatives for Level 1.

We define the Maximum Inundation Height (MIH) as our main hazard intensity metric at the coast. To estimate this metric from the offshore positions, here we employ the locally defined amplification factors obtained at Level 0. To convert the offshore quantities into MIH values, a table of pre-computed local amplification factors is used as a lookup table, according to the main wave characteristics derived at the end of STEP 2.

As an alternative metric of the coastal tsunami impact, we use Green's Law to extrapolate the maximum wave height values from 50 to 1 m depth in front of the coast.

We also provide offshore wave amplitudes as a reference.

Please note that these are not alternatives in the strict sense, since they are estimation of different tsunami metrics, not alternative approaches to the same metric approximation. Moreover, uncertainty estimation based on detailed inundation simulations presented in Section 2.3 of *Doc_P1_S1_Project_Summary* will be performed for MIH only.

Optional, inundation distance: Combine topography, empirical coastal dissipation factors, and maximum shoreline water elevation to compute a local inundation distance. Alternatively, produce maps by employing GIS inverse distance weighting extrapolation combining the above information with the STRM30+ topographical map. These possibilities are subject to consideration. Two main issues are foreseen: the difficulty of communicating the limitations inherent in such an approximated inundation distance estimation; and availability of project resources.

Level 2: Tidal stage model

The PoE elicitation (document Doc_P1_S3_Elicitation) did not recommend alternatives nor sensitivity tests for Level 2.

Tide model: we use the TPXO tool to predict tidal signal at corresponding POIs. We also calculate PDF's of the predicted tidal signal for corresponding POIs. Some details of the actual implementations have been reported in Section 2.4 of Doc_P1_S1_Project_Summary.

Level 3: Model the uncertainty on the tsunami metrics

The PoE elicitation (document Doc_P1_S3_Elicitation) recommended alternatives for Level 3 - Uncertainty modelling for tsunami hazard metrics (including uncertainties of modelling approximations from STEPS 1-3, and tides).

As discussed in the document Doc_P1_S1_Project_Summary (section 2.5.3) a new approach for dealing with the various sources of uncertainties is still under discussion in TSUMAPS-NEAM.

In alternative to this innovative approach, we plan to implement a method largely based on the log-normal sampling procedure described in Davies et al. (2016).

The results will also be tested against not including this uncertainty quantification as a sensitivity test to check the impact on the final results of choices about this level.

The details of the actual implementations of the selected models will be reported for the next review round. We also plan

2.4 STEP 4 - HAZARD AGGREGATION & UNCERTAINTY QUANTIFICATION

The PoE elicitation (document Doc_P1_S3) suggested alternatives or sensitivity tests for STEP 4 (question Q1).

For STEP 4 levels, alternatives or sensitivity tests are suggested for:

- *Level 0: Quantification of weights of the experts*
- *Level 2: Quantification of the weights of alternative models*

Alternatives and sensitivity tests can be avoided for all the other considered alternatives, that is, for the method for aggregating hazard results within each model (level 1) and for the method for integrating the alternative models into a single model (level 2).

For coherence with the other levels, the quantification of the weights of the alternative models should be considered at Level 0, instead of Level 2 as reported for the elicitation. This is also consistent with the fact that the weight values are used in the quantification of level 1. We stress that this inconsistency is only formal, and it has no impact on the results. Therefore, in the following we discuss the issue of models weights directly in Level 0.

The alternatives implemented at Levels 0 and 2 are described in what follows.

Level 0: Elicitation of experts, historical tsunami DB, paleotsunami DB

At Level 0, the PoE elicitation suggested alternatives or sensitivity tests for the quantification of weights of the experts and of models (question Q5).

In the elicitation process of PHASE 1, we weighted the experts in three different ways, that is, equal weights, performance-based weights and acknowledgement-based weights (see Doc_P1_S2 and Doc_P1_S3).

The second elicitation of the Panel of Experts (PoE) in PHASE 2 will be focused on quantifying the credibility of the different models through a weight.

In agreement with what we have done analysing the first round of elicitation of the PoE (see Doc_P1_S3), we plan to consider performance-based and acknowledgement-based weights as 2 alternative weighting schemes for experts also for the second elicitation. As a sensitivity test, we will also check the consistency of the results against the equal weights assumption.

As in PHASE 1, the elicitation will be based on a structured questionnaire provided to the TSUMAPS-NEAM Pool of Experts (PoE). The same elicitation scheme will be performed at all the levels of all the STEPs for which alternatives are available, including STEP 4 alternatives (also at this level 0).

The quantification will be based on an Analytical Hierarchical Process (AHP) procedure (Saaty 1980), which is the same method adopted in PHASE 1 (pre-assessment) – STAGE 3, as described in details in *DOC_P1_S3_Elicitation*. However, a slightly more sophisticated approach will be probably adopted in PHASE 2. In particular, the plan is to implement AHP adopting multiple criteria (yet to be defined in details), instead of using just one single criterion (personal preference) as in PHASE 1.

The model weights will be quantified directly considering the normalized scores in output from the AHP analysis of the answers of the experts. Given that 2 alternative expert weights will be implemented, we will have also two alternative quantifications of model weights.

If it will be judged feasible within TSUMAPS-NEAM, an additional quantification method will be adopted. In particular, a second quantification method can be considered by combining the expert judgements with other quantitative criteria, again adopting the AHP method. Different potential quantitative criteria may be defined, as for example the performance of models in sanity-checks, statistical tests, etc. In case, several options will be considered, leading to at least to 2 alternative methods for quantifying the weights of the alternative models. Considering the 2 alternative weights for experts and these 2 alternative procedures to quantify the weights of the models, we will reach a total of at least 4 alternative quantifications of models' weights.

This expert elicitation will be fully documented for the next review round.

As for the tsunamis datasets, we will consider the ASTARTE paleotsunami catalogue (Deliverable D2.44, http://www.astarte-project.eu/) and the Euro-Mediterranean Tsunami Catalogue, (Maramai et al. 2014). If other relevant databases will be made available, they will be considered as well.

Level 1 (combination of STEPS from 1-3)

At Level 1, the PoE elicitation did not recommend nor suggest alternatives for level 1 (question Q5).

As a consequence, we did not plan alternative, nor did sensitivity tests.

The quantification of $\lambda_{mn}(\geq H_k; POI, \Delta T)$ in each POI (as defined in STEP 2) at all the discrete tsunami intensity value H_k (as defined in STEP 3) should be in theory repeated for all the combinations of potential alternative models of STEPs 1 to 3 (identified by the indexes *m* and *n*).

Given the large number of considered alternatives. To reduce the computational effort, a Monte Carlo sampling procedure is here adopted (similarly to Selva et al., 2016). At each STEP and level, potential alternatives are sampled proportionally to their weights (the larger the weight, the higher the chance to sample for the corresponding model). Models weights emerge from Level 0. The sampling process starts from sampling the sets of weights to be used, among the alternatives

quantifications considered at STEP 4 Level 0. The corresponding set of weights will be then used for sampling the weights at all the Levels of STEPs 1 to 3.

In doing this, potential incompatibility among models will be accounted for. For example, if a 5 km cut-off for the PS/BS-only catalogue is sampled at one level, for coherence only this option should be considered in all the following levels. To allow for that, weights are sampled starting from STEP 1 – Level 1 through STEP 3 – Level 3, running first levels and then STEPs. At each sampling, only the alternative implementations which are compatible with the already sampled models will be considered, with weights re-normalized to 1. Once one model is sampled at all levels and STEPs, they are combined as in Selva et al. (2016), to produce one sample of hazard curves in each target point.

The described procedure will be performed at least 1000 times, in order to have a reasonable quantification of 16th and 84th percentiles of the epistemic uncertainty.

Level 2: Quantification of uncertainty

At Level 2, the PoE did not suggest alternative implementations nor sensitivity tests for the model for integrating the alternative models into a single ensemble model (alternative models' weights are considered at Level 0, instead of here).

As a consequence, we do not plan alternatives. Nevertheless, we plan a sensitivity test to check the unimodality of the community ensemble distribution.

The transformation of mean the annual rates $\underset{mn}{\lambda}(\geq H_k; POI, \Delta T)$ in probability will be performed by assuming a Poisson process. Given that the size of the sample of alternative models is rather large (1000 samples), we plan to produce the ensemble distribution as the empirical distribution emerging from the sample.

However, we plan to test the potential non unimodality of this distribution, in order to highlight choices that may potential lead to a separation in families of hazard curves. If distributions significantly multimodal are found, we plan to investigate which are the main alternatives that cause such separations.

The ensemble distribution will be evaluated at discrete levels of tsunami intensity, as well as, considering limits in probability values. Also, maps will be produced at predefined hazard levels, probability levels and percentiles of the epistemic uncertainty. Note that some preliminary decisions about this discretization have been reported in Section 2.5.5 of *Doc_P1_S1_Project_Summary*.

Level 3: Comparison/test with tsunami records; disaggregation

Level 3 deals with secondary results of the assessment. For this reason, it was not originally planned and thus not included into the elicitation of PHASE 1. As for level 1, we did not plan alternatives, nor sensitivity tests at this level.

For testing the results against the available tsunami records, the "community distribution" (e.g. SSHAC 1997; see also Doc_P1_S3_Elicitation) is compared with historical and paleotsunami data, in locations where enough data are available. The comparison consists of checking the compatibility of hazard curves with the observed frequency of exceedance of predefined hazard levels. An example of this comparison is reported in figure 2.10, in which we show two example of comparison, with incompatible and incompatible results (modified from ASTARTE D8.39).

Disaggregation analyses will be also performed in several key POIs. Disaggregation against magnitudes and regions are foreseen (e.g., like in Selva et al., 2016). The details of disaggregation within TSUMAPS are still under discussion, since they depend on the availability of resources.

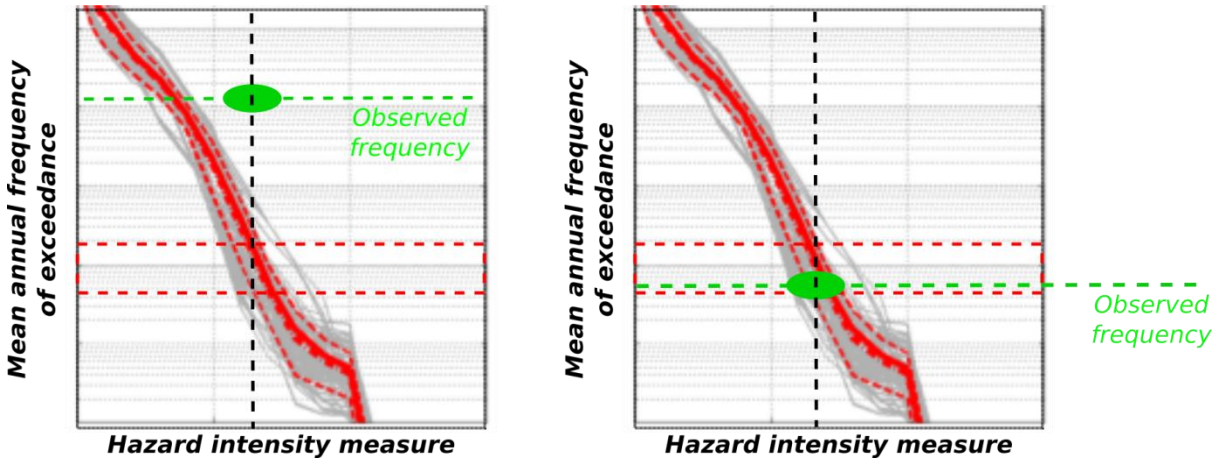

Figure 2.10: comparison scheme between the hazard curve and its epistemic uncertainty (red lines) and the observation from historical or paleotsunami records, modified from ASTARTE D8.39). Given one hazard intensity level (black dashed line), the observed frequency is computed by counting the number of non-overlapping ΔT in the past with exceedance of a given hazard threshold, divided by the total number of ΔT for which the information (exceedance / non exceedance) exists. The observation dots are plotted considering the potentially large uncertainty in measuring MIH in past observation over rather large areas. The acceptability bounds (horizontal red dashed lines) are set considering both the epistemic uncertainty on the hazard curves (red dotted lines) for the same intensity level of the observation point.

References

Basili R., Kastelic V., Demircioglu M. B., Garcia Moreno D., Nemser E. S., Petricca P., Sboras S. P., Besana-Ostman G. M., Cabral J., Camelbeeck T., Caputo R., Danciu L., Domac H., Fonseca J., García-Mayordomo J., Giardini D., Glavatovic B., Gulen L., Ince Y., Pavlides S., Sesetyan K., Tarabusi G., Tiberti M. M., Utkucu M., Valensise G., Vanneste K., Vilanova S., Wössner J. (2013). The European Database of Seismogenic Faults (EDSF) compiled in the framework of the Project SHARE. *http://diss.rm.ingv.it/share-edsf/*, doi: 10.6092/INGV.IT-SHARE-EDSF.

Basili R, Volpe M, Maesano FE, Tiberti MM, Lorito S, Romano F, Tonini R (2017). Influence of seismogenic source geometrical accuracy on PTHA: a test case for the Calabrian subduction interface, Geophysical Research Abstracts, Vol. 19, EGU2017-18872-1, EGU General Assembly 2017.

Berryman K., Wallace L., Hayes G., Bird P., Wang K., Basili R., Lay T., Pagani M., Stein R., Sagiya T., Rubin C., Barreintos S., Kreemer C., Litchfield N., Stirling M., Gledhill K., Haller K., Costa C. (2015). The GEM Faulted Earth Subduction Interface Characterisation Project, Version 2.0, April 2015, GEM Faulted Earth Project, available from http://www.nexus.globalquakemodel.org/gem-faulted-earth/posts.

Bird, P. (2003) An updated digital model of plate boundaries, Geochem Geophys Geosys 4(3), 1027, doi:10.1029/2001GC000252.

Blaser, L., Krüger, F., Ohrnberger, M., Scherbaum, F., 2010. Scaling relations of earthquake source parameter estimates with special focus on subduction environment. Bulletin of the Seismological Society of America 100, 2914-2926, doi: 10.1785/0120100111.

Bommer JJ (2012). Challenges of Building Logic Trees for Probabilistic Seismic Hazard Analysis, EARTHQUAKE SPECTRA, Vol: 28, 1723-1735, ISSN: 8755-2930.

Davies G, Griffin J, Løvholt F, Glymsdal S, Harbitz C, Thio HK, Lorito S, Basili R, Selva J, Geist E, Baptista MA (2017). A global probabilistic tsunami hazard assessment from earthquake sources. From: Scourse, E. M., Chapman, N. A., Tappin, D. R. & Wallis, S. R. (eds) Tsunamis: Geology, Hazards and Risks. Geological Society, London, Special Publications, 456, https://doi.org/10.1144/SP456.5.

de la Asunción, M., Castro, M. J., Fernández-Nieto, E. D., Man- tas, J. M., Ortega Acosta, S., and González Vida, J. M.: Efficient GPU implementation of a two waves TVD-WAF method for the two-dimensional one layer shallow water system on structured meshes, Comput. Fluids, 80, 441–452, 2013.

Delavaud E., Cotton F., Akkar S., Scherbaum F., Danciu L., Beauval C., Drouet S., Douglas J., Basili R., Sandikkaya M., Segou M., Faccioli E., Theodoulidis N. (2012). Toward a ground-motion logic tree for probabilistic seismic hazard assessment in Europe. Journal of Seismology, 16(3), 451-473, doi: 10.1007/s10950-012-9281-z.

Dziewonski, A.M., T.A. Chou, and J.H. Woodhouse (1981). Determination of earthquake source parameters from waveform data for studies of global and regional seismicity, Journal of Geophysical Research, 86(B4), 2825, doi: 10.1029/JB086iB04p02825.

Ekström, G., M. Nettles, and A.M. Dziewoński (2012). The global CMT project 2004–2010: Centroid-moment tensors for 13,017 earthquakes, Physics of the Earth and Planetary Interiors, 200-201, 1-9, doi:10.1016/j.pepi.2012.04.002.Geist, E. & Parsons, T., 2006. Probabilistic analysis of tsunami hazards, *Nat. Hazards,* 37, 277–314.

Eshelby, J. The determination of the elastic field of an ellipsoidal inclusion and related problems. Proc. Roy. Soc. London, Series A 241, 376–396. doi: 10.1098/rspa.1957.0133 (1957).

Grünthal G. and R. Wahlström (2012). The European-Mediterranean Earthquake Catalogue (EMEC) for the last millennium. Journal of Seismology, 16, 535-570, doi 10.1007/s10950-012-9302-y.

Hanks, T.C., Bakun, W.H., 2008. M-logA Observations for Recent Large Earthquakes. Bulletin of the Seismological Society of America 98, 490-494, doi: 10.1785/0120070174.

Hayes, G. P., Wald, D. J. & Johnson, R. L. (2012) Slab1.0: A three-dimensional model of global subduction zone geometries. Journal of Geophysical Research: Solid Earth 117, n/a-n/a, doi: 10.1029/2011jb008524.

Herrero, A. & Bernard, P. A Kinematic Self-Similar Rupture Process for Earthquakes. Bull. Seismol. Soc. Am. 84(No. 4), 1216–1228 (1994).

Herrero A., Murphy S., Complex slip distributions on complex fault geometries. SSA meeting, Denver 17-21 april. (2017).

Herrero A, Murphy S, Lorito S, Romano F, Volpe M (2017). The influence of complex fault geometry and slip of large subduction earthquakes on tsunami generation, Geophysical Research Abstracts Vol. 19, EGU2017-14724-1, EGU General Assembly 2017.

ISC - International Seismological Centre (2014), On-line Bulletin, http://www.isc.ac.uk, Internatl. Seismol. Cent., Thatcham, United Kingdom.

Kagan, Y.Y., Bird, P., Jackson, D.D. (2010) Earthquake Patterns in Diverse Tectonic Zones of the Globe, Pure Appl. Geophys., 167(6), 721-741, doi:10.1007/s00024-010-0075-3.

Keller M., Pasanisi A., Marcilhac M., Yalamas T., Secanell R., and Senfaute G. (2014), A Bayesian Methodology Applied to the Estimation of Earthquake Recurrence Parameters for Seismic Hazard Assessment, Qual. Reliab. Engng. Int., 30, 921–933, doi: 10.1002/qre.1735

Kajiura, K. (1963). The leading wave of a tsunami, Bull. Earthquake Res. Inst. Univ., Tokyo, 41, 535–571.

Lay, T., Kanamori, H., Ammon, C.J., Koper, K.D., Hutko, A.R., Ye, L., Yue, H., Rushing, T.M., 2012. Depth-varying rupture properties of subduction zone megathrust faults. J. Geophys. Res. 117, B04311. http://dx.doi.org/10.1029/2011JB009133.

Leonard, M., 2014. Self-Consistent Earthquake Fault-Scaling Relations: Update and Extension to Stable Continental Strike-Slip Faults. Bulletin of the Seismological Society of America, doi: 10.1785/0120140087.

Lorito, S.,Selva J., Basili R., Romano, F., Tiberti, M. M.,and Piatanesi, A (2015). Probabilistic Hazard for Seismically-Induced Tsunamis: Accuracy and Feasibility of Inundation Maps, Geophys. J. Int., 200, 574–588.

Maramai A., Brizuela B., Graziani L. (2014). The Euro-Mediterranean Tsunami Catalogue, Annals of Geophysics, 57, 4, S0435; doi:10.4401/ag-6437.

Maesano F.E., Tiberti M.M., Basili R., (2017). The Calabrian Arc: three-dimensional modelling of the subduction interface. Sci. Rep., under review.

Marzocchi, W., Taroni, M., Selva, J., 2015. Accounting for epistemic uncertainty in PSHA: logic tree and ensemble modeling. Bulletin of the Seismological Society of America, 105(4), 2151-2159.

Meade, B. J. (2007), Algorithms for the calculation of exact displacements, strains, and stresses for triangular dislocation elements in a uniform elastic half space, Comput. Geosci., 33, 1064–1075, doi:10.1016/j.cageo.2006.12.00.

Molinari I, Tonini R, Lorito S, Piatanesi A, Romano F, Melini D, Hoechner A, Gonzàlez Vida JM, Maciás J, Castro MJ, de la Asunción M (2016). Fast evaluation of tsunami scenarios: uncertainty assessment for a Mediterranean Sea database, Nat. Hazards Earth Syst. Sci., 16, 2593-2602, doi: 10.5194/nhess16-2593-2016.

Murotani, S., Miyake, H., Koketsu, K., 2008. Scaling of characterized slip models for plate-boundary earthquakes. Earth Planets Space 60, 987-991, doi.

Murotani, S., Satake, K., Fujii, Y., 2013. Scaling relations of seismic moment, rupture area, average slip, and asperity size forM~9 subduction-zone earthquakes. Geophysical Research Letters 40, 5070-5074, doi: 10.1002/grl.50976.

Murphy, S. et al. Shallow slip amplification and enhanced tsunami hazard unravelled by dynamic simulations of mega-thrust earthquakes. Sci. Rep. 6, 35007; doi: 10.1038/srep35007 (2016).

Nosov, M.A. & Kolesov, S.V. (2011). Optimal Initial Conditions for Simulation of Seismotectonic Tsunamis, Pure Appl. Geophys. 168: 1223, doi: 10.1007/s00024-010-0226-6.

Novotni, M. & Klein, R. Computing geodesic distances on triangular meshes. The 10-th International Conference in Central Europe on Computer Graphics, Visualization and Computer Vision 2002 (WSCG 2002).

Okada, Y. (1992). Internal deformation due to shear and tensile faults in a half-space, Bull. Seismol. Soc. Am., 82, 1018–1040.

Pondrelli S. and Salimbeni S. (2015). Regional Moment Tensor Review: An Example from the European Mediterranean Region. In Encyclopedia of Earthquake Engineering (pp. 1-15), http://link.springer.com/referenceworkentry/10.1007/978-3-642-36197-5_301-1, Springer Berlin Heidelberg.

Ruiz, J. A., Baumont, D., Bernard, P. & Berge-Thierry, C. Modelling directivity of strong ground motion with a fractal, k− 2, kinematic source model. Geophys. J. Int. 186, 226–244, doi: 10.1111/j.1365- 246X.2011.05000.x (2011).

Saaty, T.L., 1980. The Analytic Hierarchy Process: Planning, Priority Setting, Resource Allocation, ISBN 0-07-054371-2, McGraw-Hill.

Selva J., Tonini R., Molinari I., Tiberti M.M., Romano F., Grezio A., Melini D., Piatanesi A., Basili R., Lorito S. (2016). Quantification of source uncertainties in Seismic Probabilistic Tsunami Hazard Analysis (SPTHA). Geophys. J. Int., 205, 1780-1803, doi:10.1093/gji/ggw107.

Selva J, Lorito S, Basili R, Tonini R, Tiberti MM, Romano F, Perfetti P, Volpe M (2017). On the use of faults and background seismicity in Seismic Probabilistic Tsunami Hazard Analysis (SPTHA), Geophysical Research Abstracts Vol. 19, EGU2017-17395-1, EGU General Assembly 2017.

Stucchi, M., A. Rovida, A.A. Gomez Capera, P. Alexandre, T. Camelbeeck, M.B. Demircioglu, P. Gasperini , V. Kouskouna, R.M.W. Musson, M. Radulian, K. Sesetyan, S. Vilanova, D. Baumont, H. Bungum, D. Faeh, W. Lenhardt, K. Makropoulos, J.M. Martinez Solares, O. Scotti, M. Zivcic, P. Albini, J. Batllo, C. Papaioannou, R. Tatevossian, M. Locati, C. Meletti, D. Viganò and D. Giardini (2012). The SHARE European Earthquake Catalogue (SHEEC) 1000-1899. Journal of Seismology, doi 10.1007/s10950-012-9335-2.

SSHAC (Senior Seismic Hazard Analysis Committe), 1997. Recommendations for probabilistic seismic hazard analysis: Guidance on uncertainty and use of experts, U.S. Nuclear Regulatory Commission Report NUREG/CR-6372.

Storchak, D.A., D. Di Giacomo, I. Bondár, E. R. Engdahl, J. Harris, W.H.K. Lee, A. Villaseñor and P. Bormann, 2013. Public Release of the ISC-GEM Global Instrumental Earthquake Catalogue (1900-2009). Seism. Res. Lett., 84, 5, 810-815, doi: 10.1785/0220130034.

Strasser, F.O., Arango, M.C., Bommer, J.J., 2010. Scaling of the source dimensions of interface and intraslab subduction-zone earthquakes with moment magnitude. Seismological Research Letters 81, 941-950, doi: 10.1785/gssrl.81.6.941.

Weichert DH. (1980) Estimation of the earthquake recurrence parameters for unequal observation periods for different magnitudes. Bulletin of the Seismological Society of America; 70:1337–1356.

Wells, D.L., Coppersmith, K.J., 1994. New empirical relationships among magnitude, rupture length, rupture width, rupture area, and surface displacement. Bull. Seismol. Soc. Am. 84, 974-1002, doi.

Woessner J., Danciu L., Giardini D., Crowley H., Cotton F., Grünthal G., Valensise G., Arvidsson R., Basili R., Demircioglu M., Hiemer S., Meletti C., Musson R.W., Rovida A., Sesetyan K., Stucchi M., and the SHARE consortium. (2015). The 2013 European Seismic Hazard Model - Key Components and Results. Bulletin of Earthquake Engineering, 13, 3553-3596, doi: 10.1007/s10518-015-9795-1.

Zheng, Y. H., Anderson, J. G. & Yu, G. A Composite Source Model for Computing Realistic Synthetic Strong Ground Motions. Geophys. Res. Lett 21, 725–728, doi: 10.1029/94GL00367 (1994).